ENLIL: Modeling of Heliospheric Space Weather

Dusan Odstrcil

George Mason University & NASA/GSFC

CCMC Workshop, Key Largo, FL, January 16-20, 2012

Acknowledgements

Collaboration on various applications with:
AFRL: Nick Arge
CCMC: MacNeice, Sandro Taktakishvili, Antti Pulkinnen
GMU: Jie Zhang
NOAA/SWPC: Chris Balch, Leslie Mayer, Vic Pizzo
NRL: Arnaud Thernissien, Alexis Rouillard
SAIC: Jon Linker, Zoran Mikic, Peter Riley
UCB: Steve Ledvina, Christina Lee, Janet Luhmann
UCSD: Bernie Jackson, Paul Hick, Mario Bisi
UNH: Jimmy Raeder

This work has been supported in part by AFOSR/MURI, NASA/LWS, NASA/STEREO, NASA/HGI, NSF/CISM, and NSF/SHINE projects.

Calibration of Background Solar Wind

Ambient Solar Wind

Near Solar Minimum

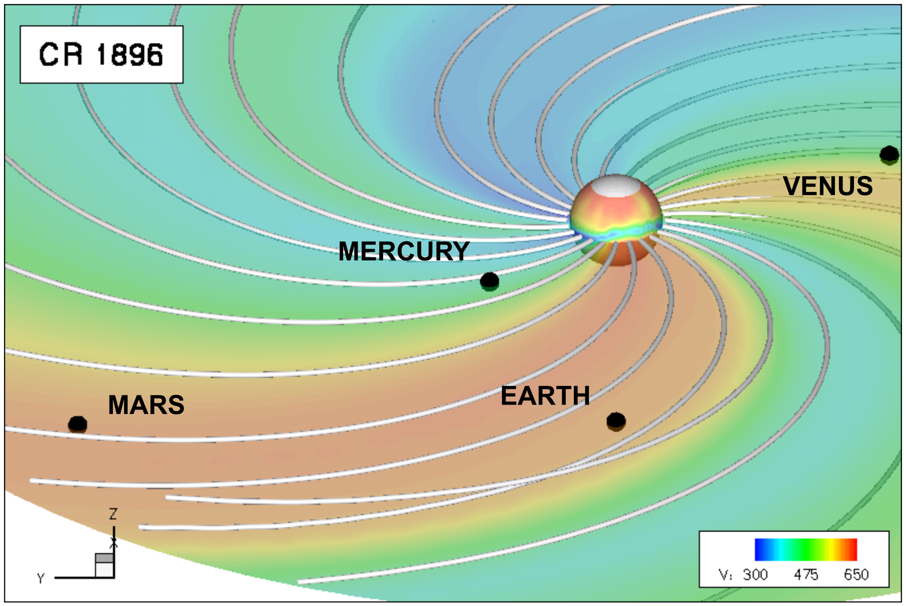

Near Solar Maximum

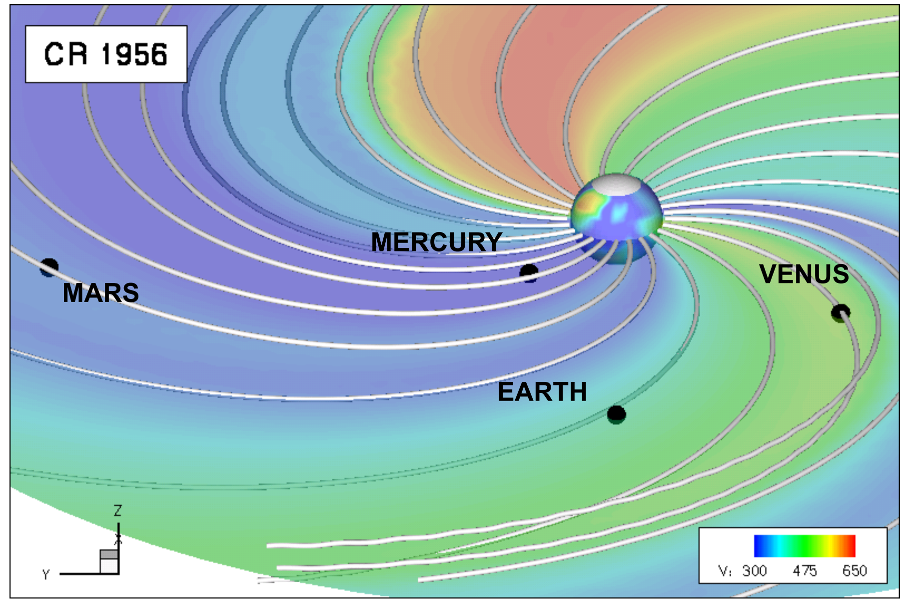

Model Boundary

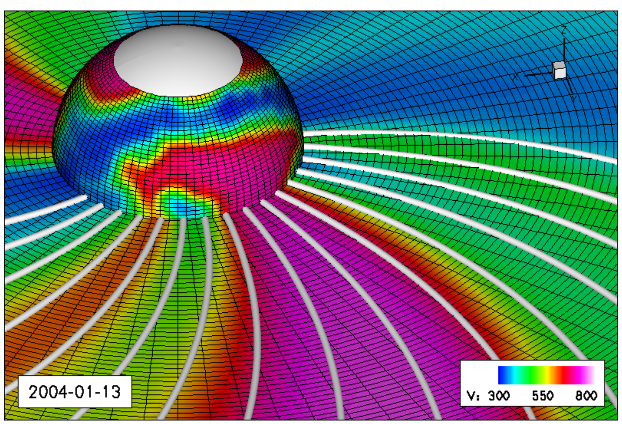

Inner Heliosphere

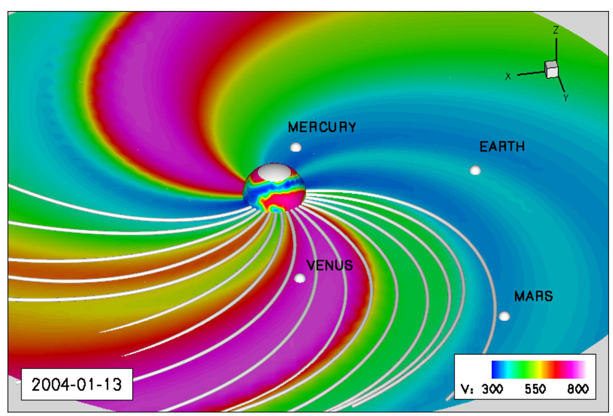

Outer Heliosphere

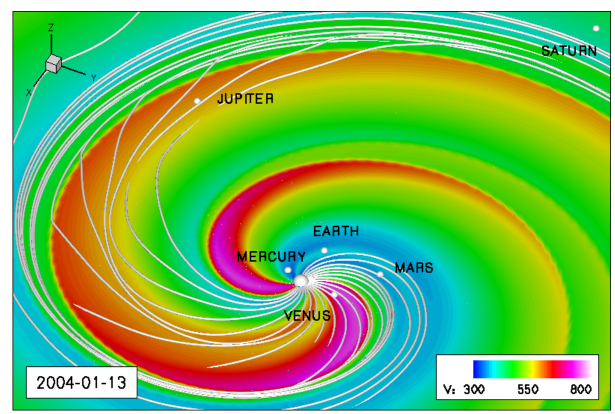

Driving ENLIL by Different Coronal Models

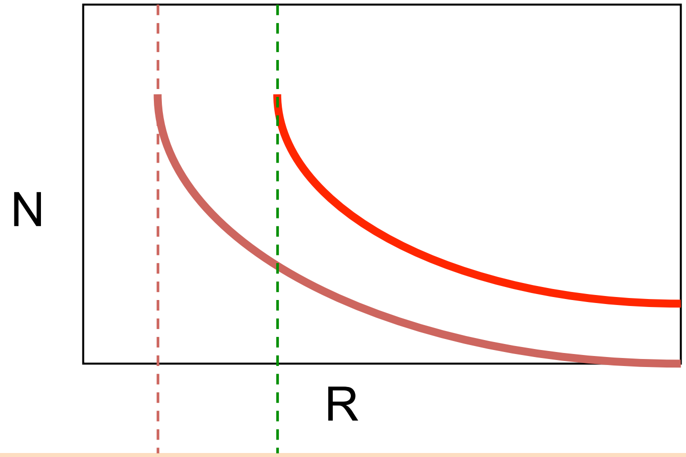

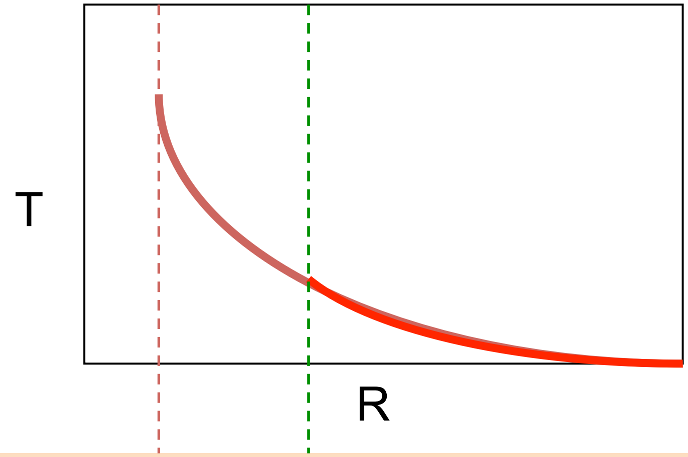

Free parameters depend on the position of the inner boundary

	WSA – 0.1 AU	MAS – 0.14 AU
Dfast (cm-3)	200	100
Tfast (MK)	1.0	0.6
Bfast (nT)	300	150
Vfast (km/s)	650	675
Vred (km/s)	30	20
Shift (deg)	8	12

Calibration of Input Data for ENLIL Runs

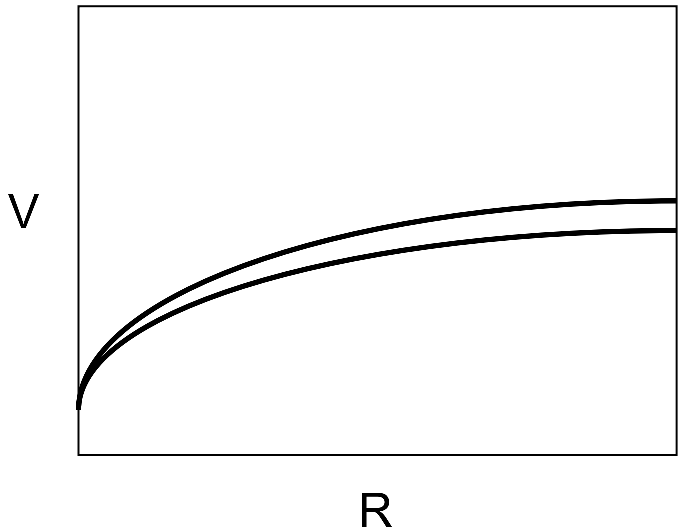

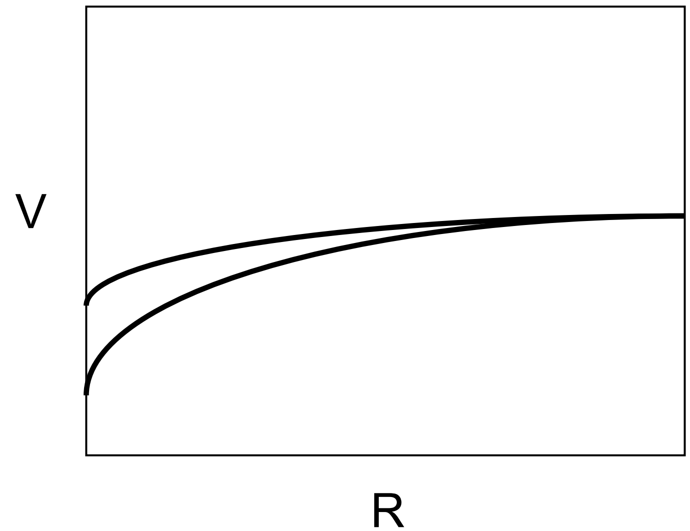

Solar wind expands: parameters at Earth depends on the coronal temperature, ratio of specific heats, and on initial speed.

- Fast-stream solar wind proton number density (D_{fast} = 300 cm^{-3})
- Fast-stream solar wind mean temperature (T_{fast} = 1 MK)
- Ratio of specific heats (g = 1.5)
- Ratio of alpha particles (a = 0)
- Momentum flux balance: NV^{X} (x = 2)
- Pressure balance (P_{the} = const)

Solar Wind – MASFR – NSO: 2005

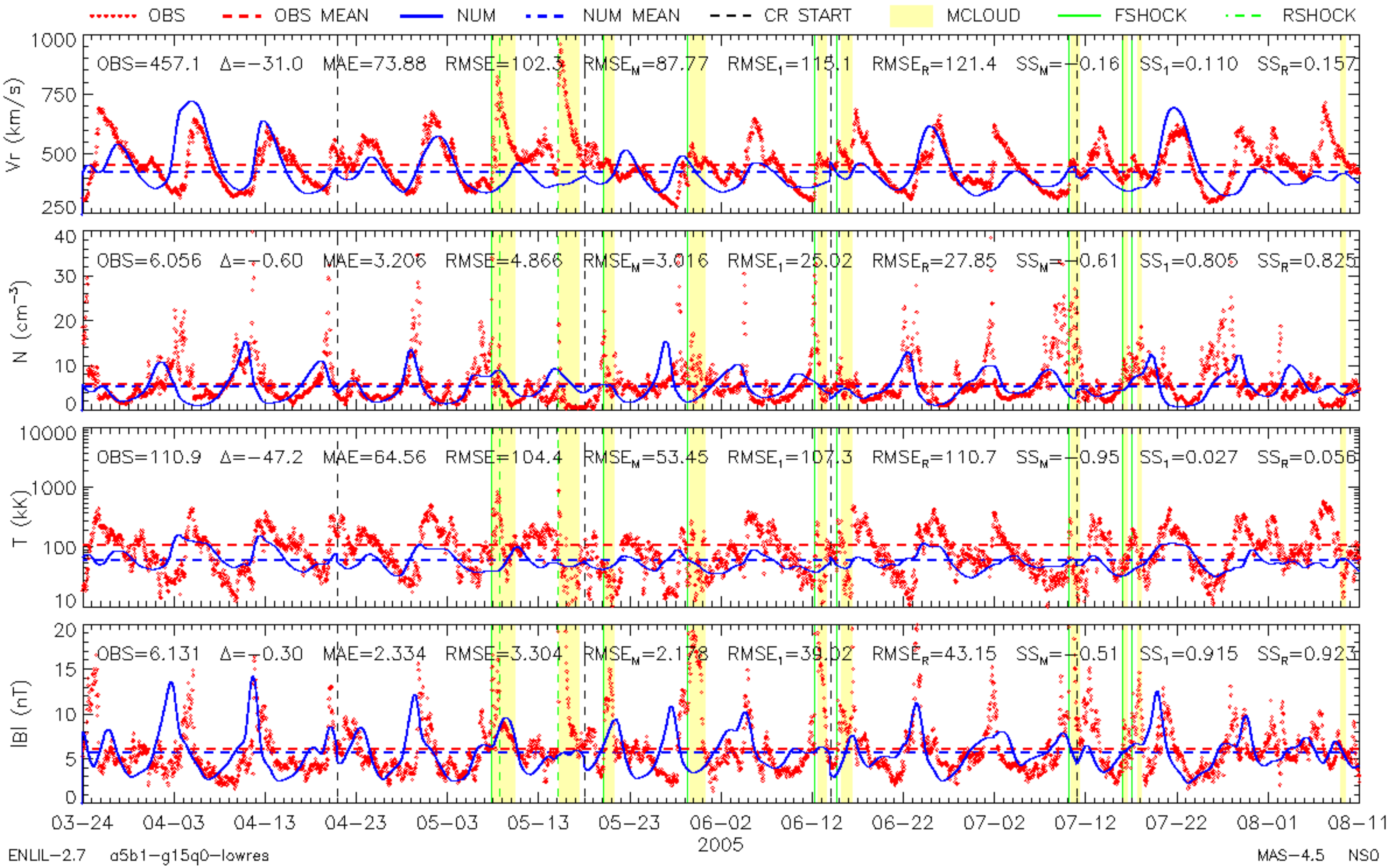

Solar Wind – WSAFR – NSO: 2005

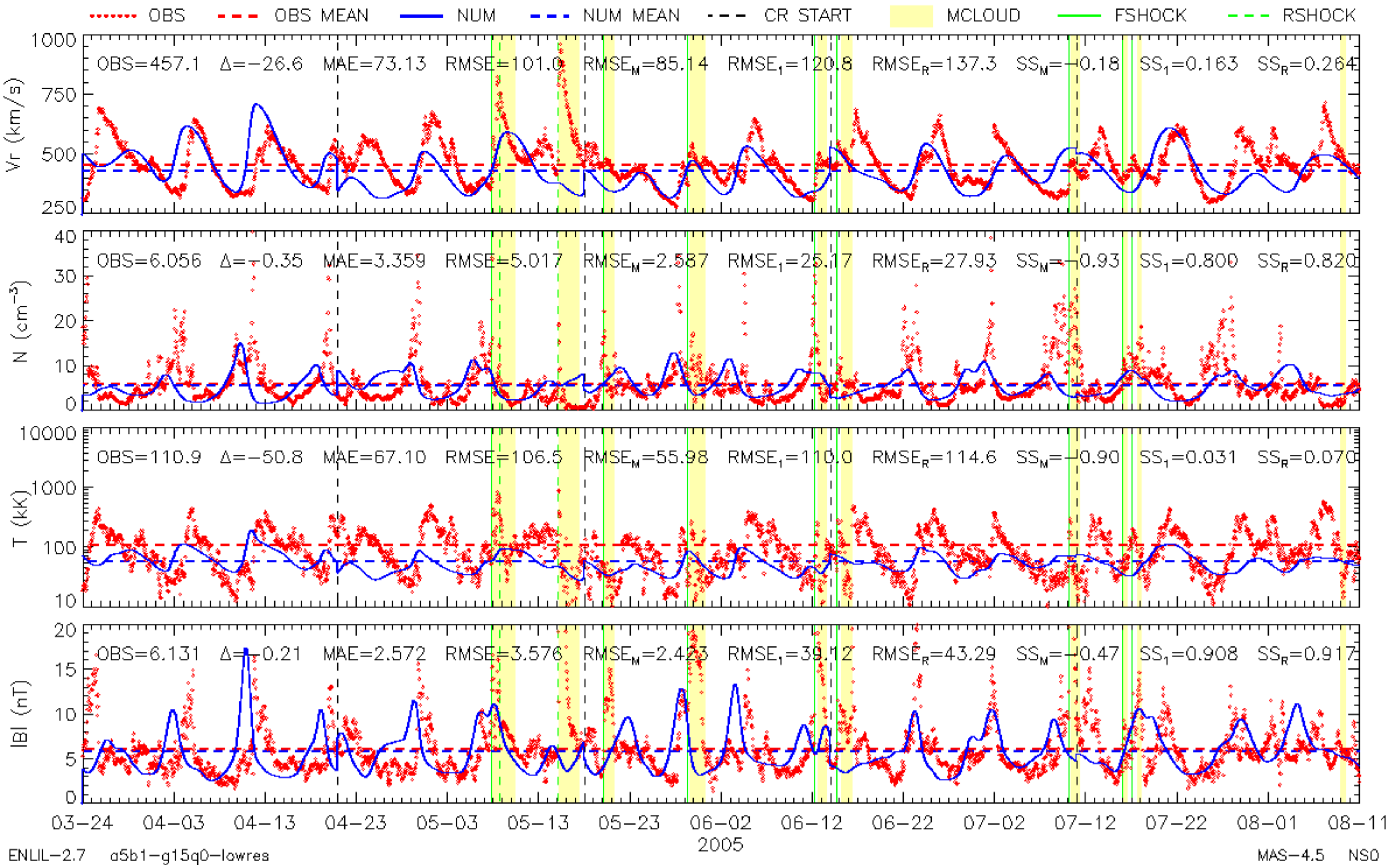

Solar Wind Velocity – Skill Scores

	Mean value	1-day persistency	27-days recurrence
MASFR-NSO(1)	-0.16	0.110	0.157
WSAFR-NSO(1)	-0.18	0.163	0.264
WSAFR-MD(1)	-0.14	0.078	0.210
WSADU-GONG(2)			
(1) 2005: CRs 2028-2932 (2) 2007: 12 months			

- Shift In stream arrival times causes large errors and predictions are worse than using the mean value
- All numerical predictions are better than using the 1-day or 27-days earlier values
- Periods affected by transient disturbances will be removed from analysis
- <u>Results were achieved by using different parameters for different coronal models and different solar observatories</u>
- Further improvement of coronal models and tuning of heliospheric code is needed

Adjusting the WSA Velocity at R_{BND}

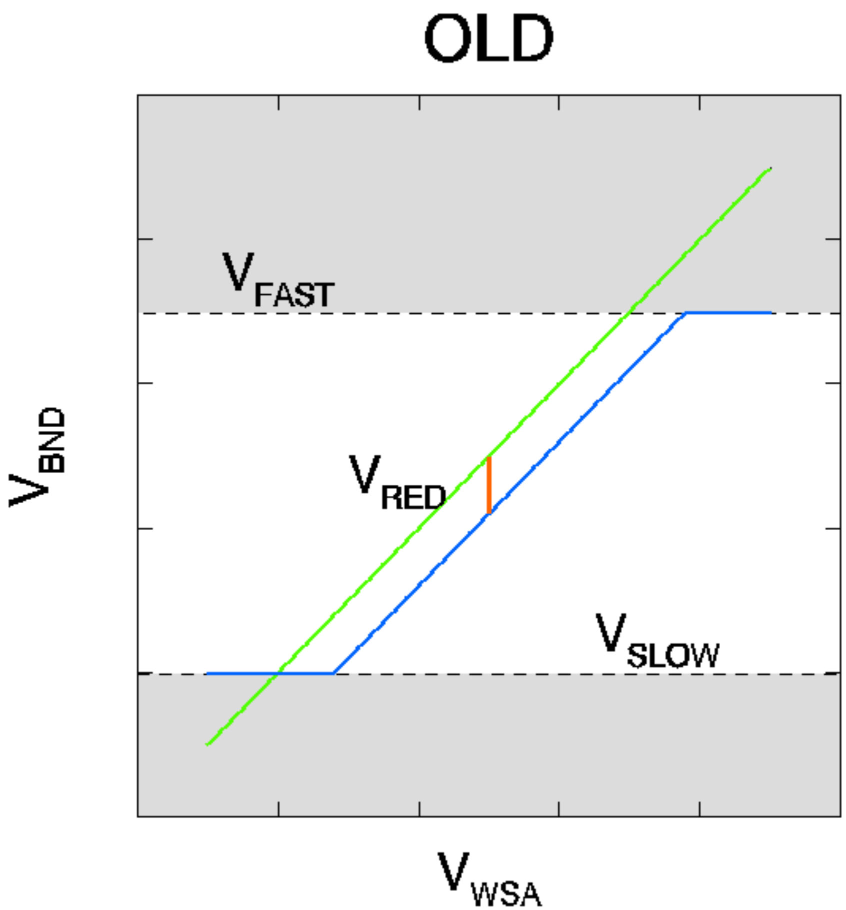

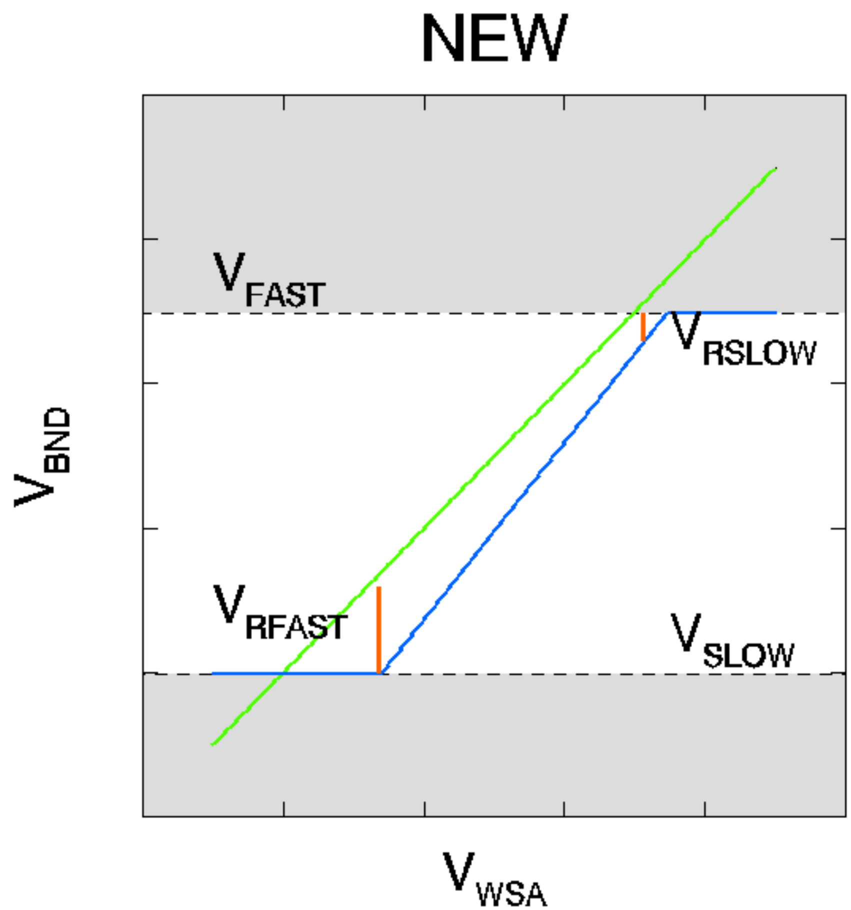

- GREEN – WSA velocity is used as is
- BLUE – WSA velocity is reduced and clipped

SW Velocity Prediction in Synodic Frame

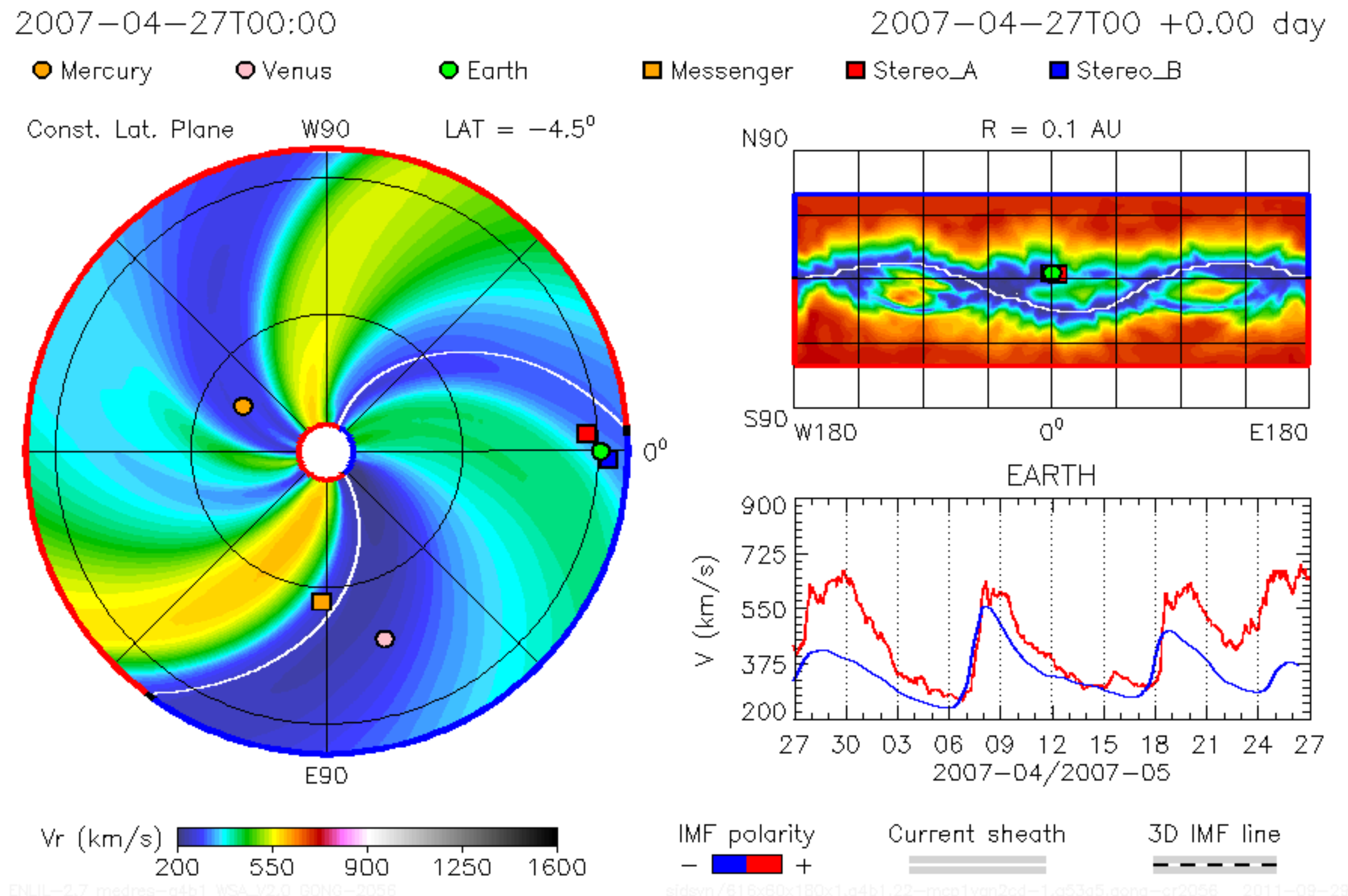

SW Velocity Prediction in Sidereal Frame

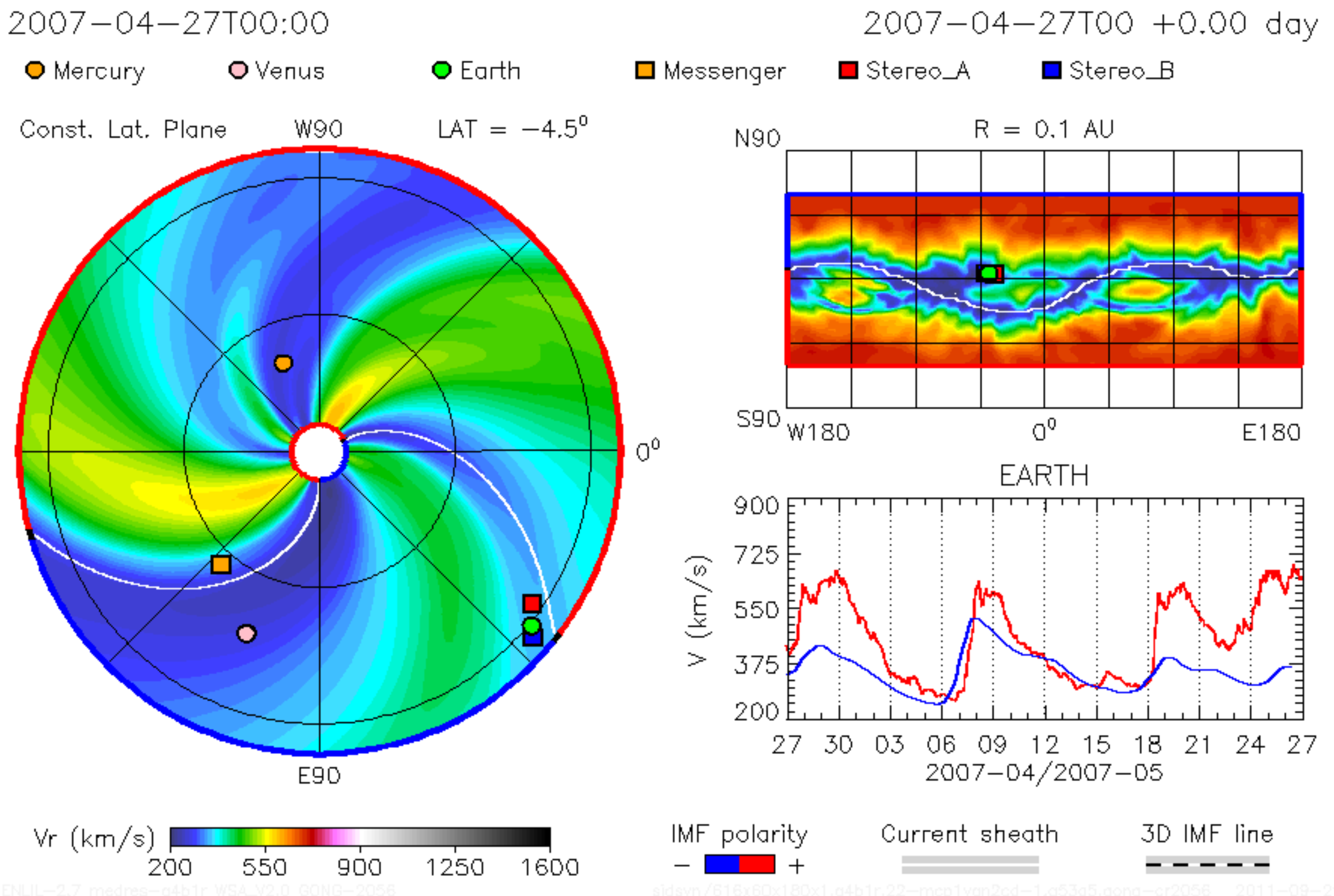

Simulating Time Periods by Relevant CR Maps

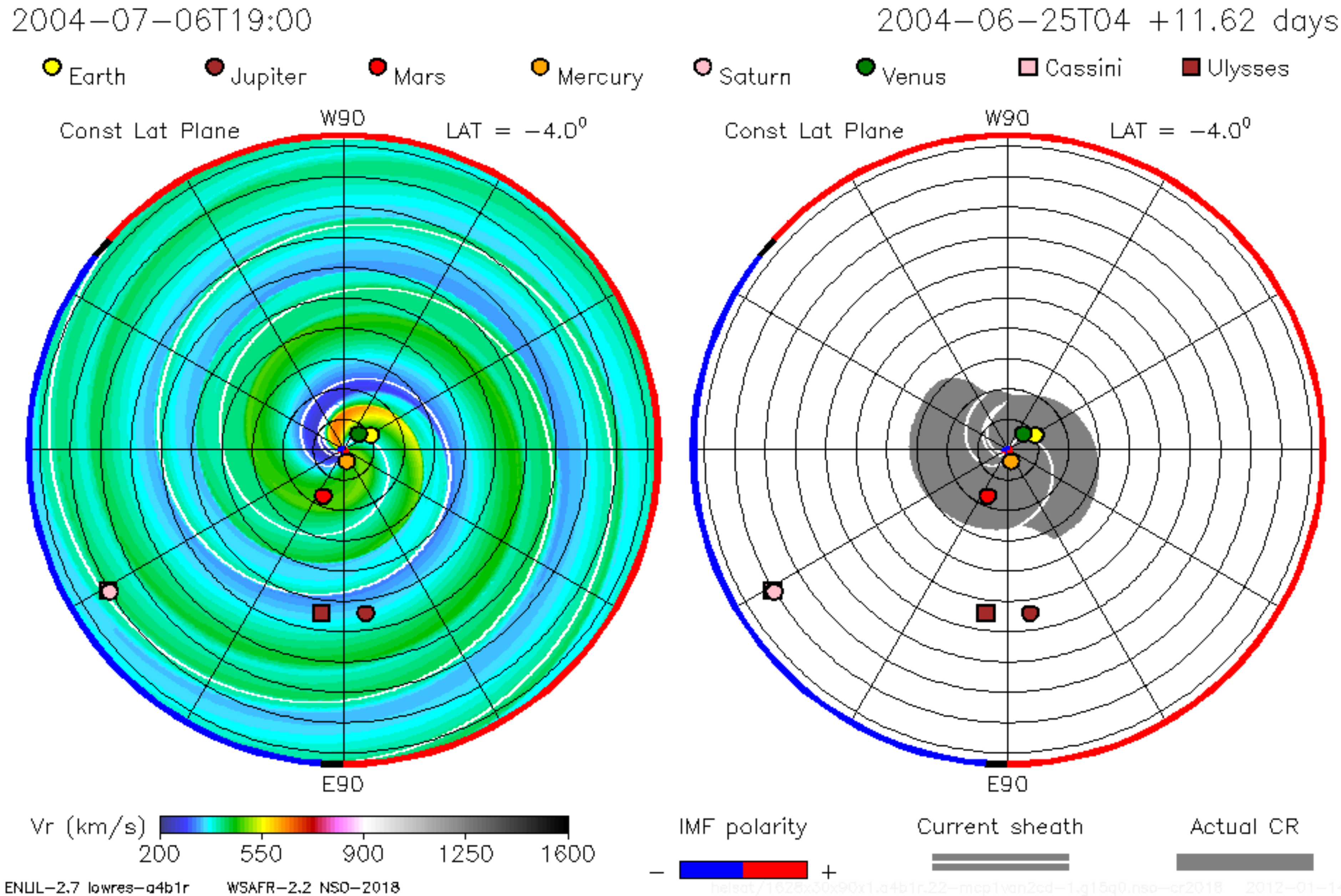

Simulating Time Periods by Relevant CR Maps

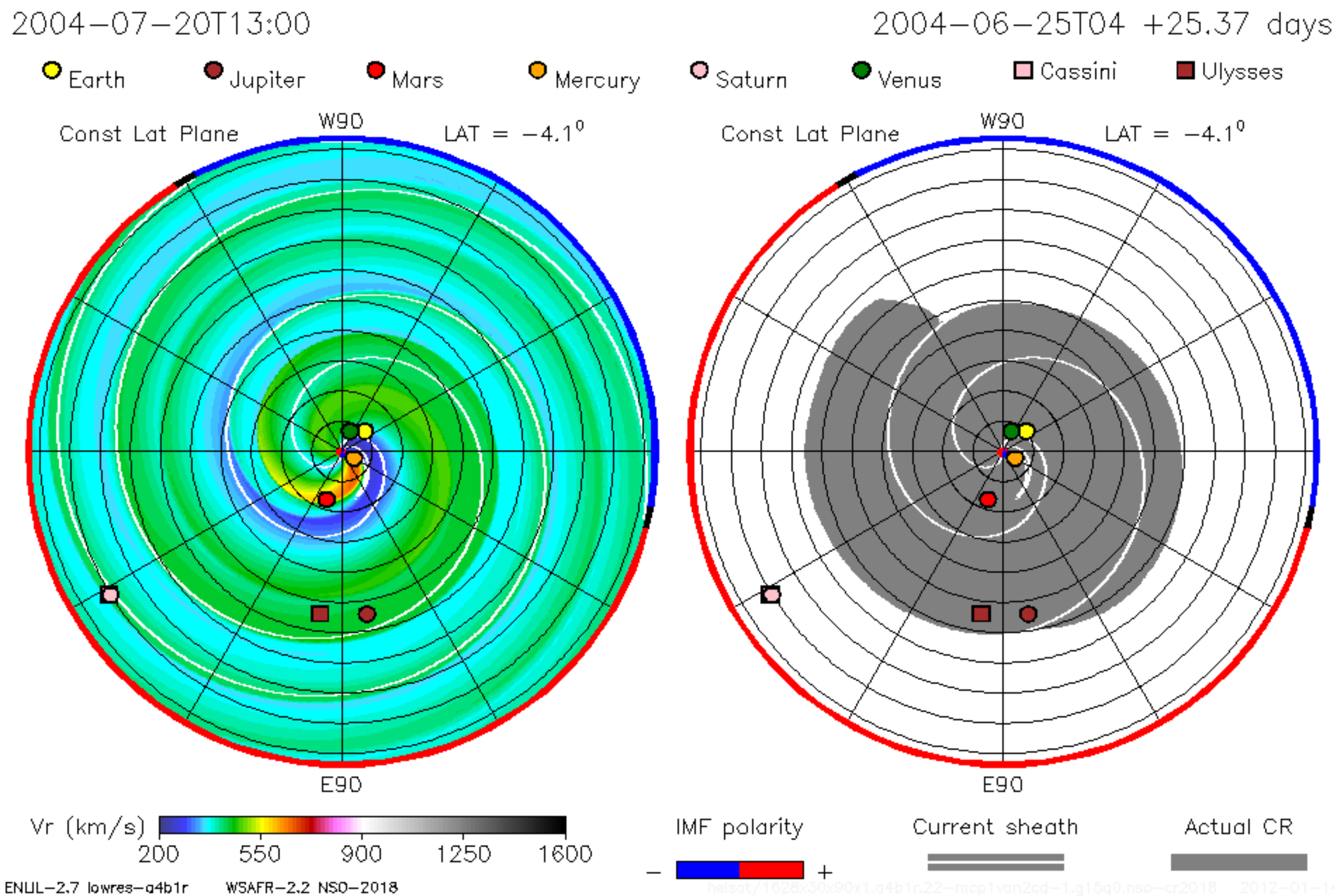

Simulating Time Periods by Relevant CR Maps

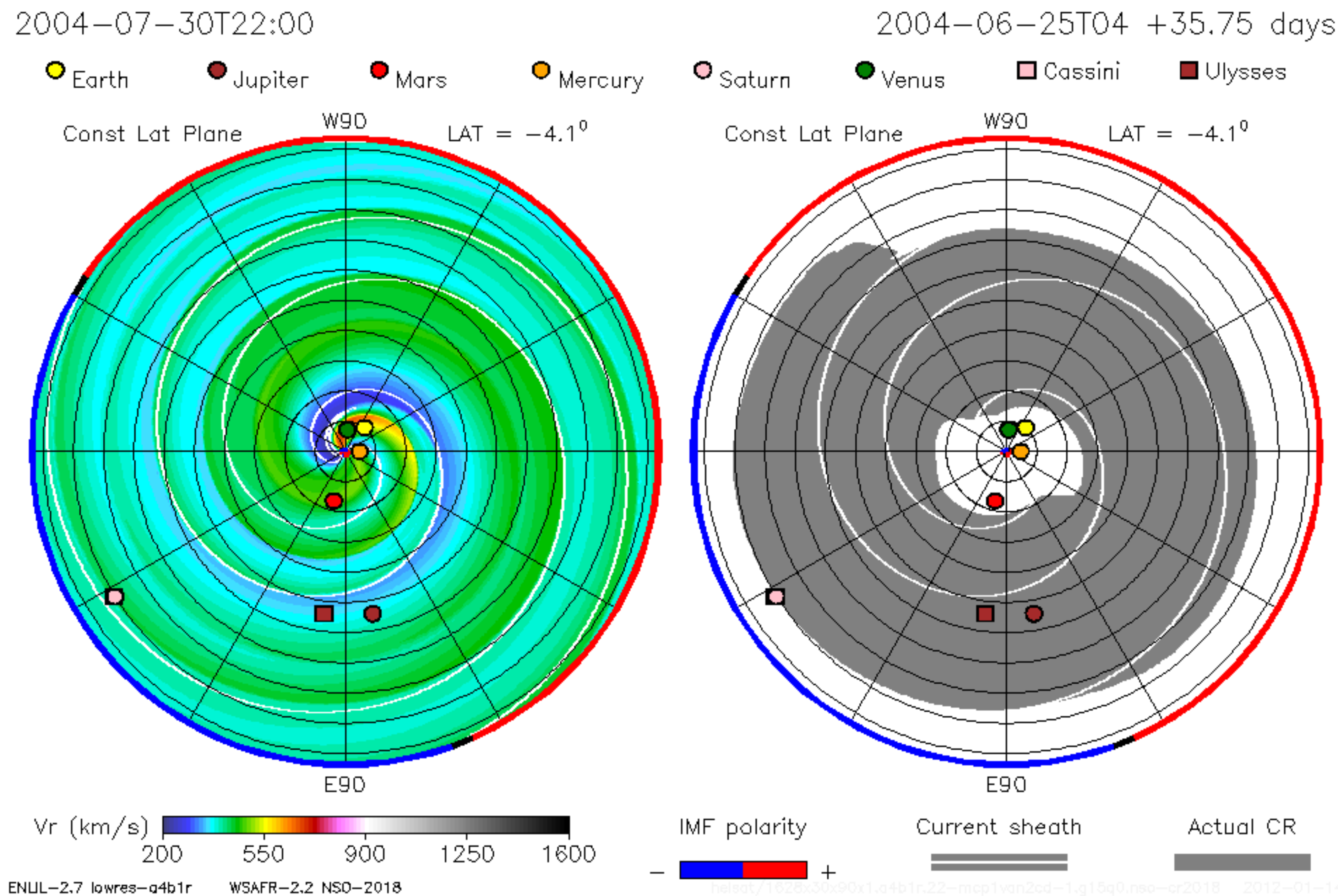

Simulating Time Periods by Relevant CR Maps

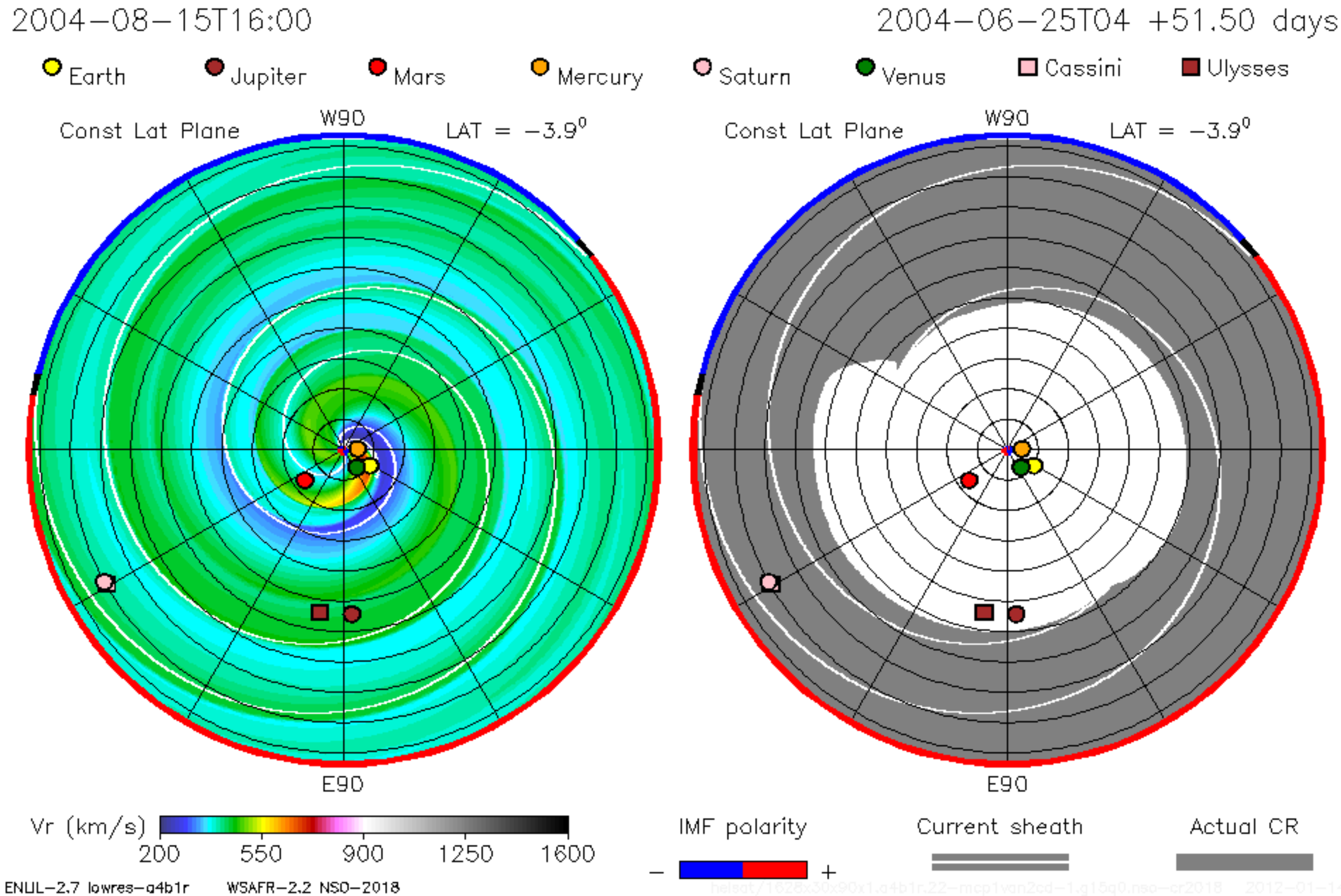

Improved Coronal Model and Evolving SW

Air Force Data Assimilative Photospheric Flux Transport (ADAPT) Model

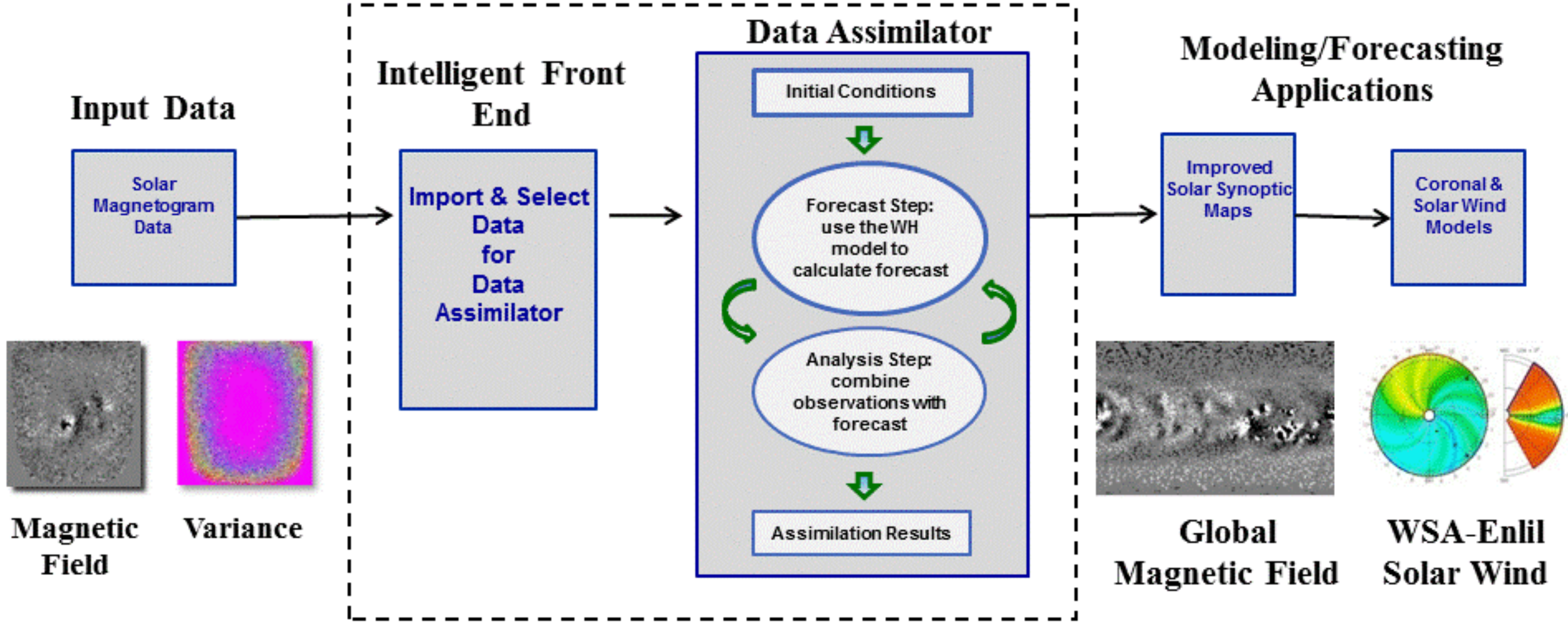

Diagram of the general data flow and processing of ADAPT: the Intelligent Front End imports and selects the best available magnetogram data, along with estimated uncertainties, to be assimilated by the ensemble least-squares (EnLS) method with the latest WH flux transport map of the global solar magnetic field. These maps are then used as input for coronal and solar wind models, e.g., WSA-ENLIL (Odstrcil et al., 2005).

Simulation of Transient Disturbances

CME "Cone" Model

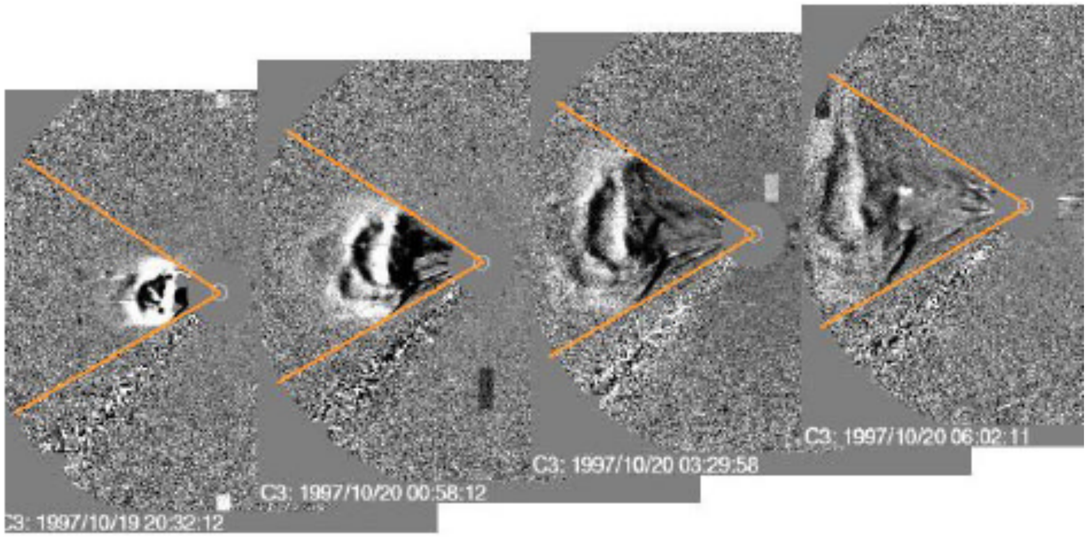

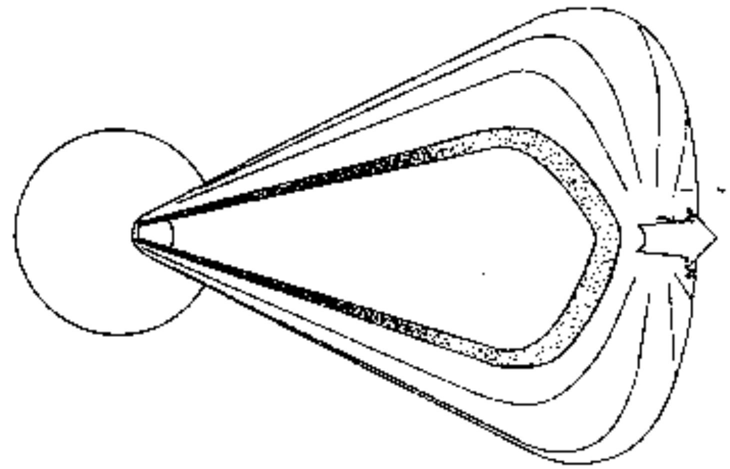

<u>Observational evidence:</u>

- CME expands self-similarly
- Angular extent is constant

<u>Conceptual model:</u>

- CME as a shell-like region of enhanced density

[*Howard et al,* 1982; *Fisher & Munro,* 1984]

Transient Disturbances

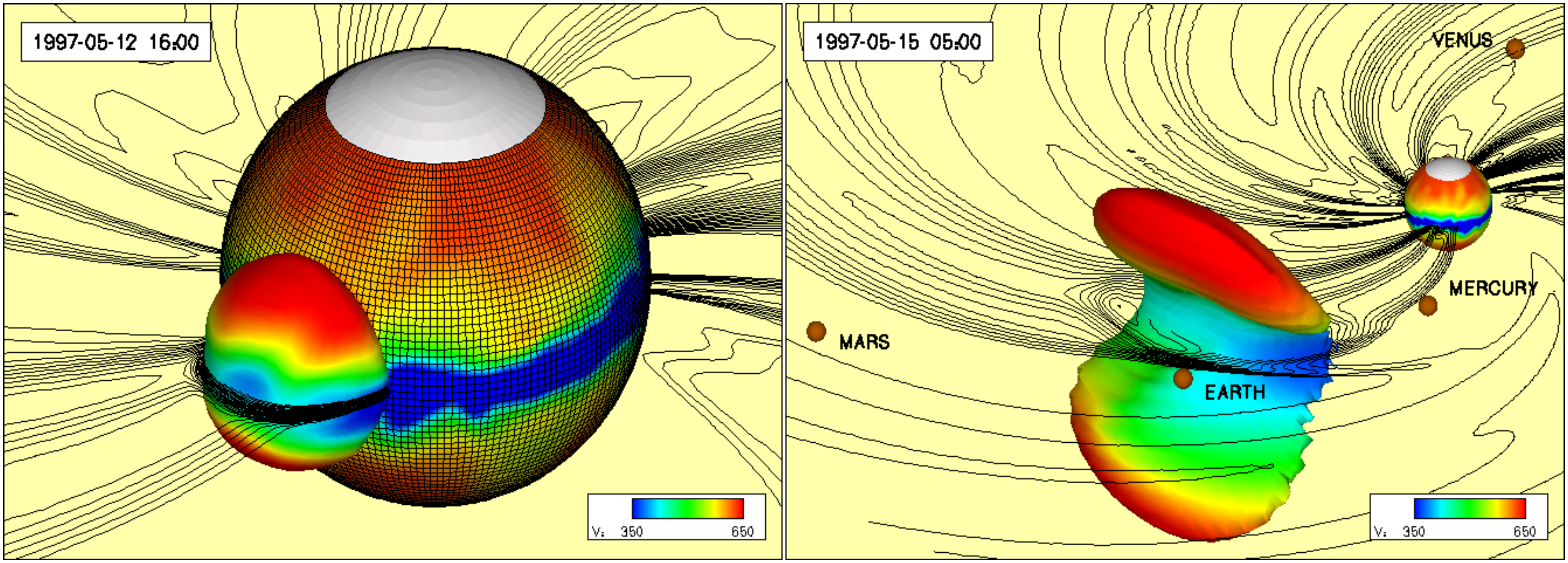

Modeling of the origin of CMEs is still in the research phases and it is not expected that real events can be routinely simulated in near future. Therefore, we have developed an intermediate modeling system which uses the WSA coronal maps, fitted coronagraph observations, specifies 3D ejecta, and drives 3D numerical code ENLIL.

Verification and Validation

CME arrival time prediction: comparison to Gopalswamy's empirical model

2-nd reference model: Gopalswamy et al. 2001 empirical model for CME transit time:

$$T_{transition} = \frac{-u + \sqrt{u^2 + 2ad_1}}{a} + \frac{d_2}{\sqrt{u^2 + 2ad_1}}$$

$$a = 2.193 - 0.0054 \cdot u$$

Here: u is the observed initial velocity of the CME at $2R_S$, d_1 runs through 3 values 0.76,0.86 and 0.95 AU and d_2=1AU - d_1. This defines the prediction window for the CME arrival time to the Earth. For our comparison we used the mean of the prediction window for the 13 events we studied.

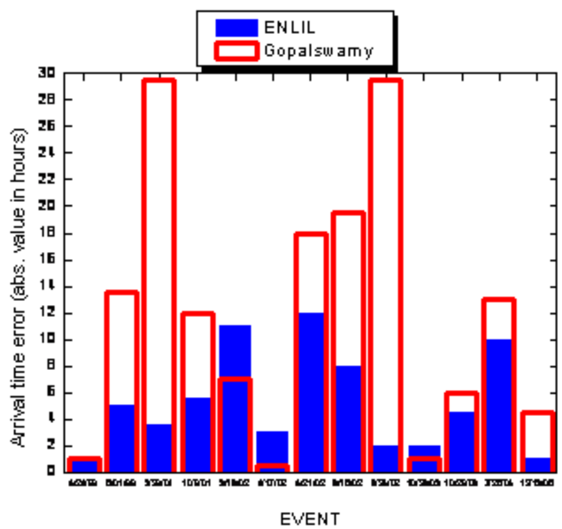

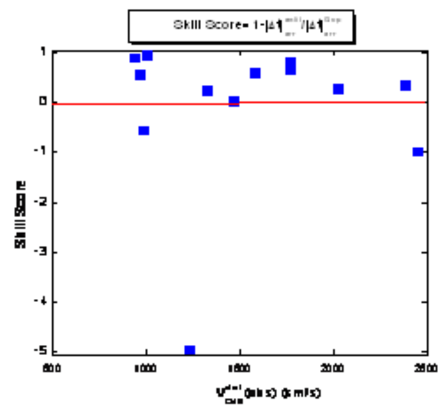

Skill score w/respect to the Gopalswamy's empirical model

$$\textit{Skill Score} = 1 - \frac{\left| t^{arr}_{enlil} - t^{arr}_{obs} \right|}{\left| t^{arr}_{Gopal} - t^{arr}_{obs} \right|}$$

ENLIL does better job than Gopalswamy's model in 10 out of 13 cases

Earth-Connected IMF Line with Two Shocks

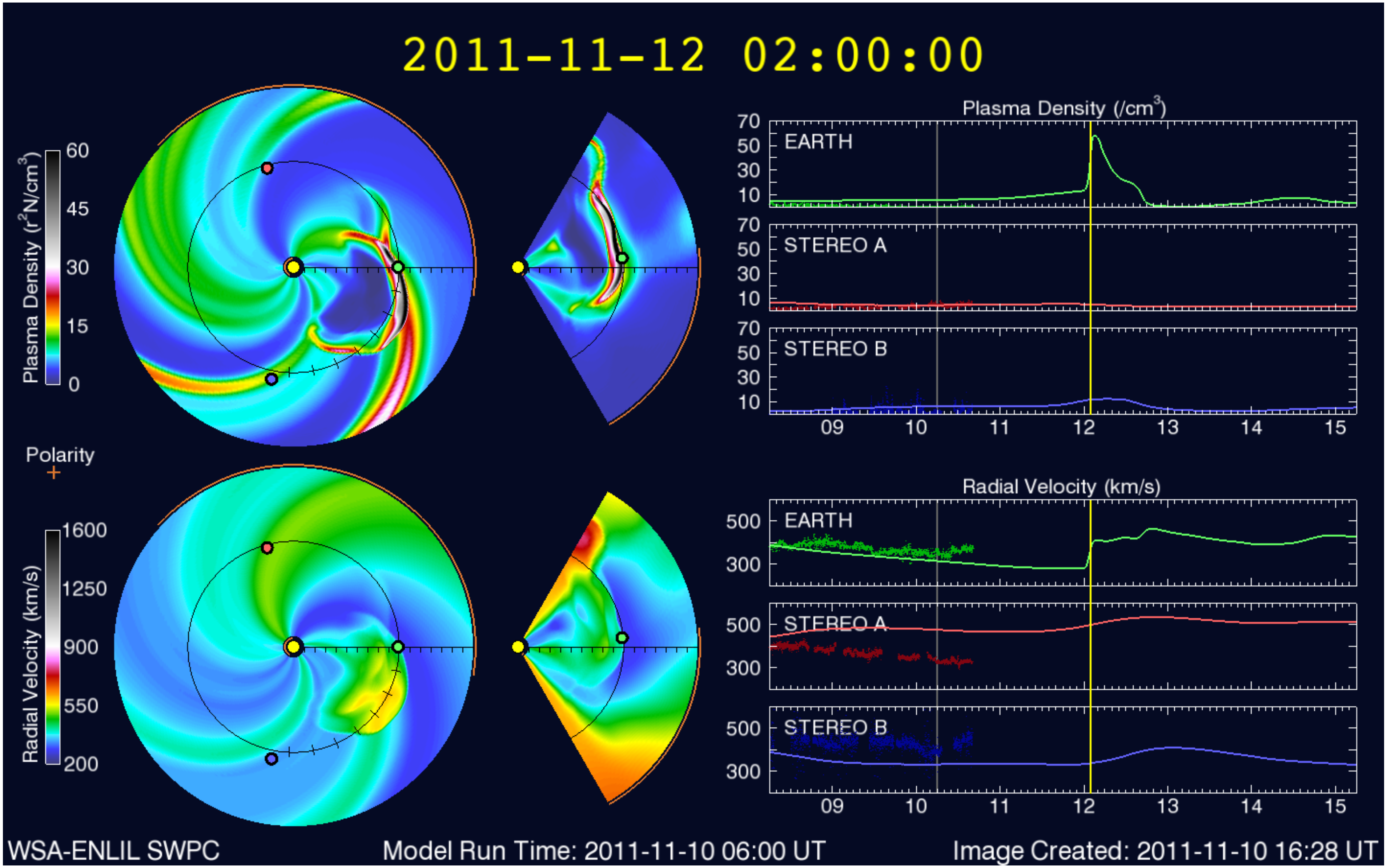

CME Analyzing Tool at SWPC

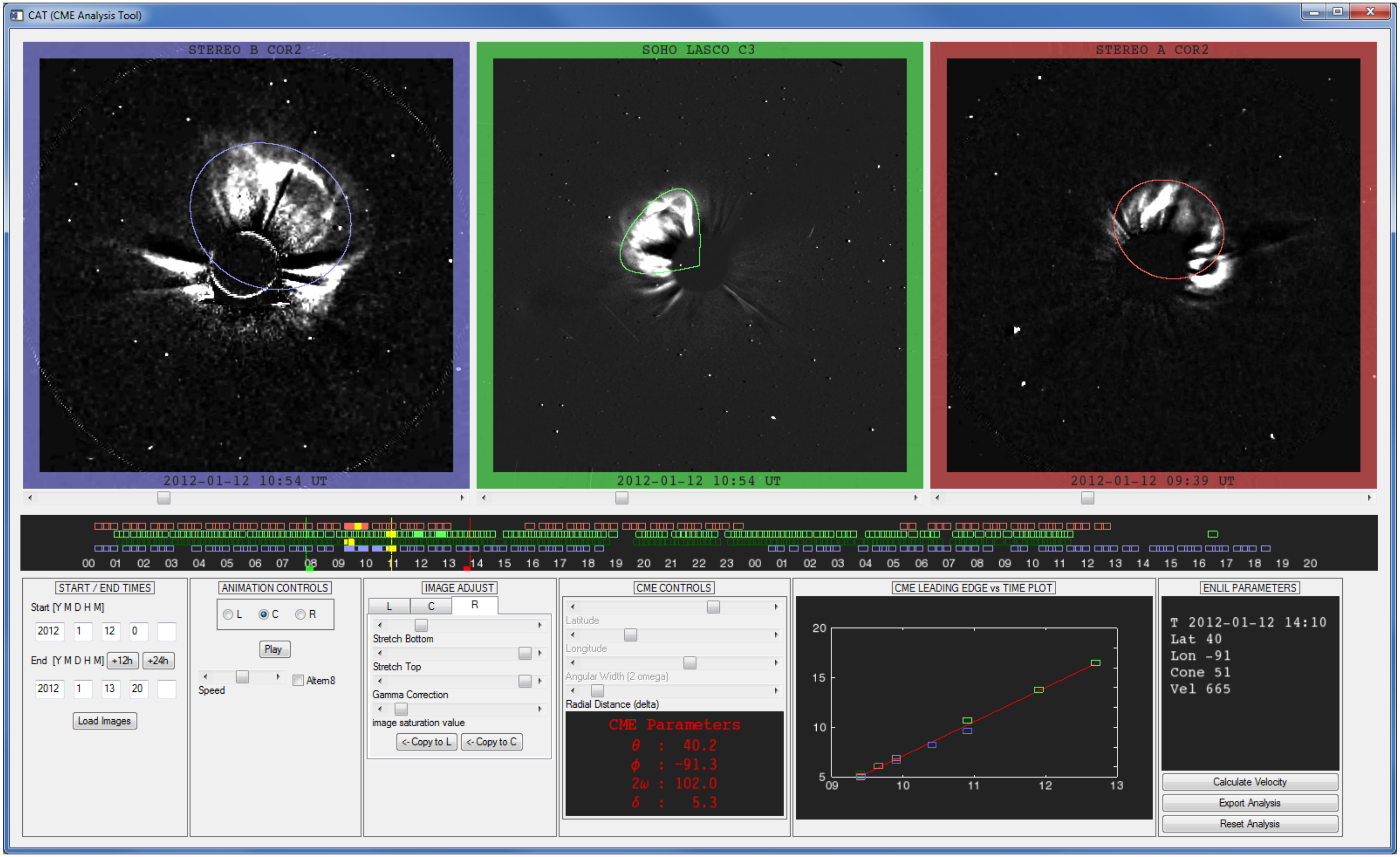

Interpretation of Remote Observations

Boundary Conditions – Velocity (GLT)

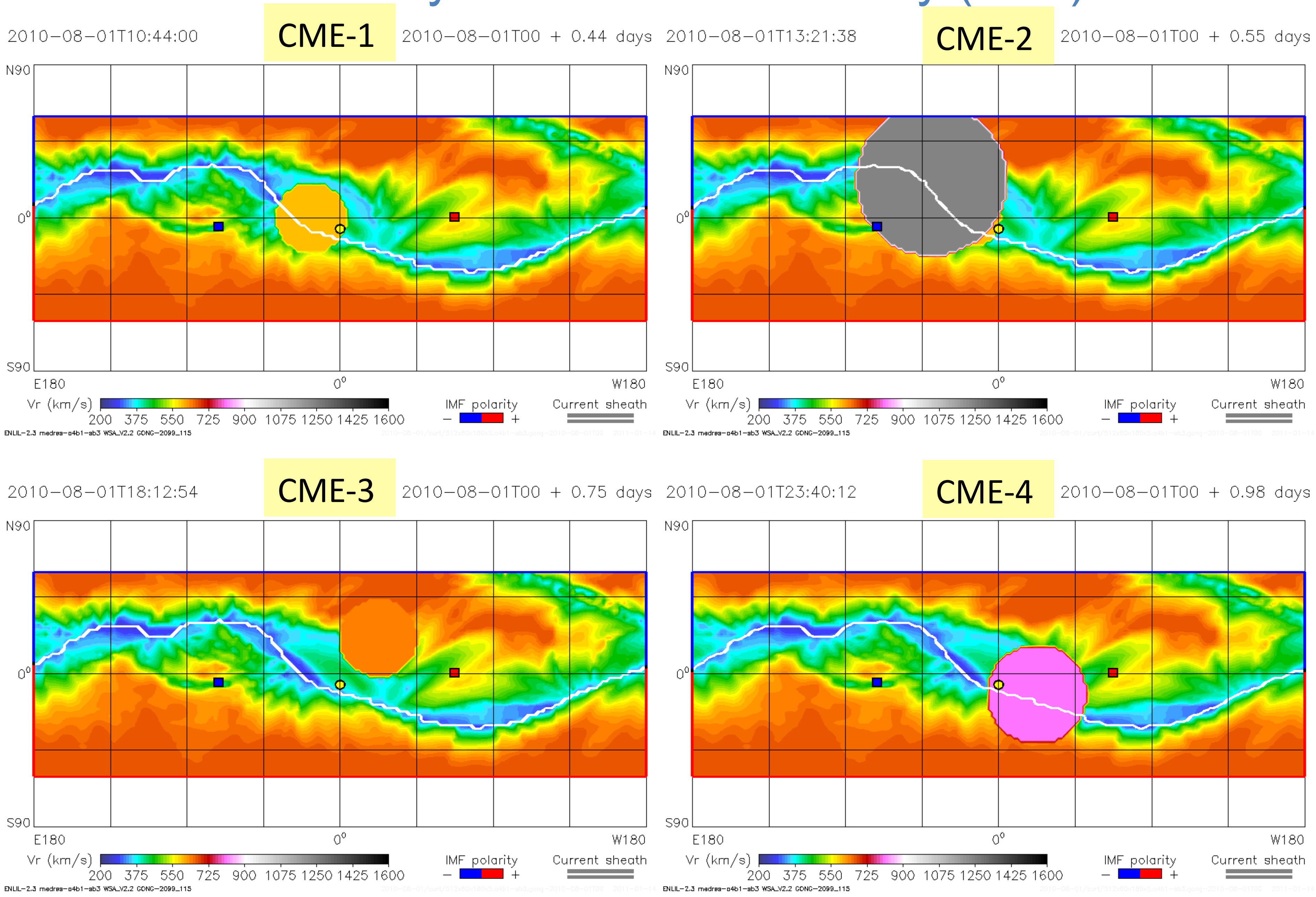

Shocks and CMEs in the Inner Heliosphere

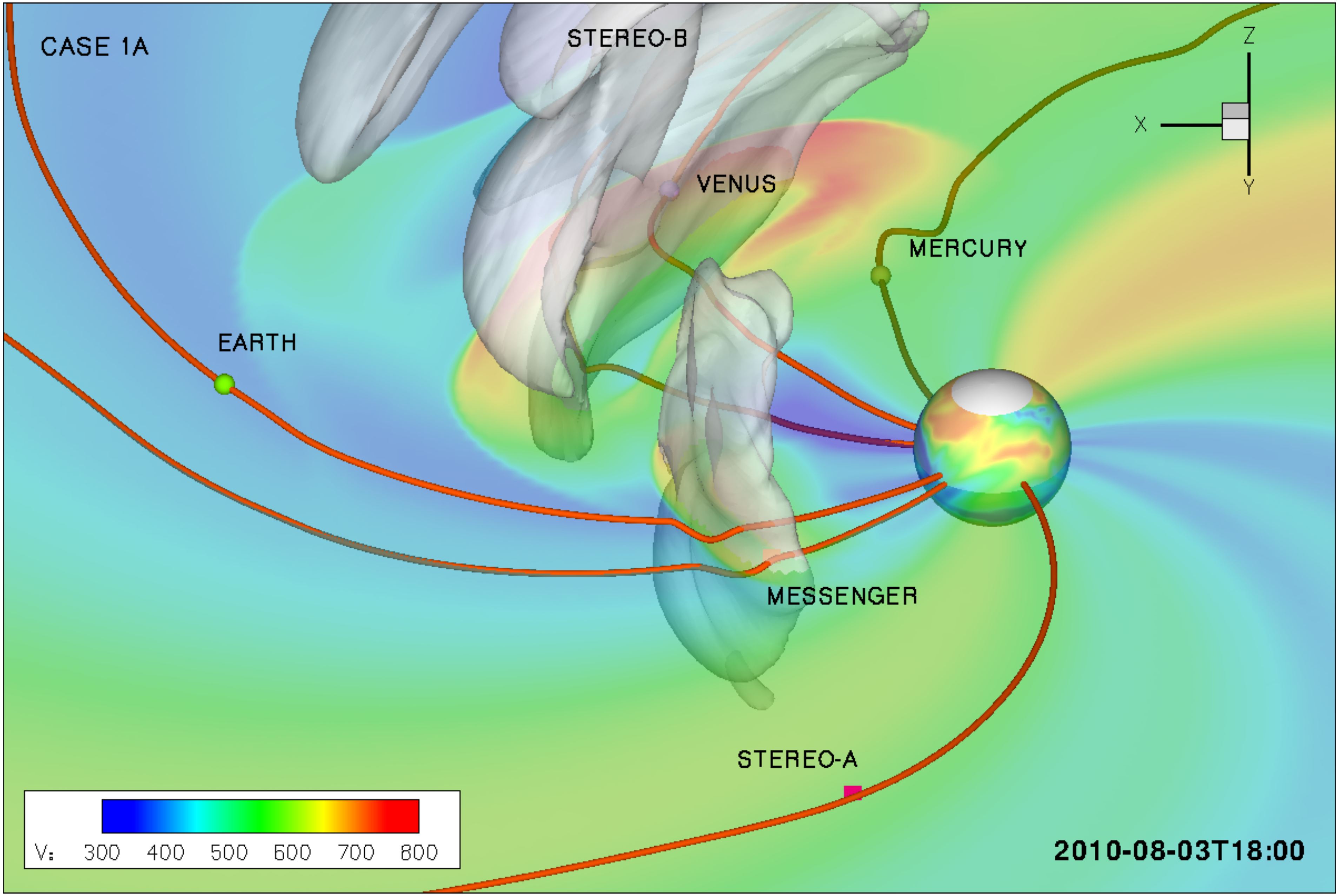

Temporal Profiles – Earth (Case 2)

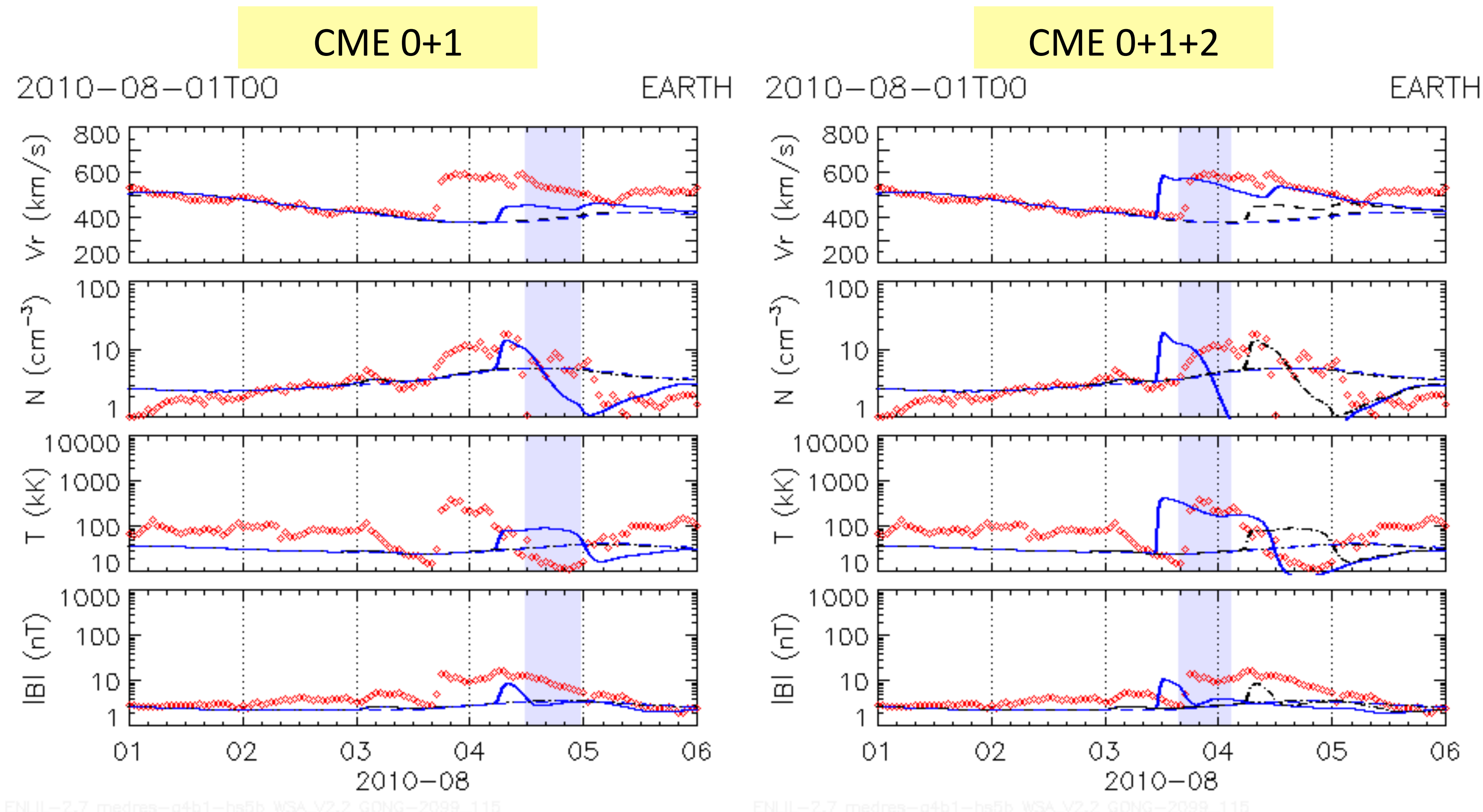

- CME-0 expansion causes only a weak wave with small effect at Earth
- CME 2 completely overtakes CME-1
- CME-1 and CME-2 have ejecta at Earth

Temporal Profiles – Earth (Case 2)

CME 0+1+2+3

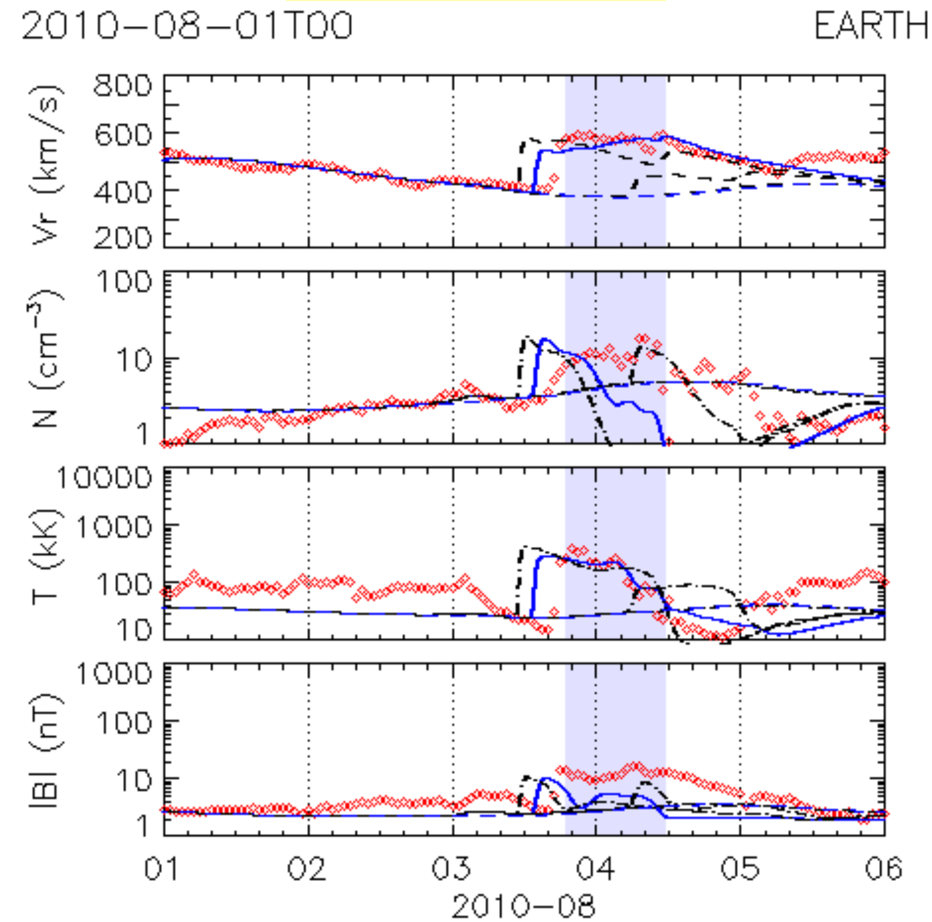

CME 0+1+2+3+4

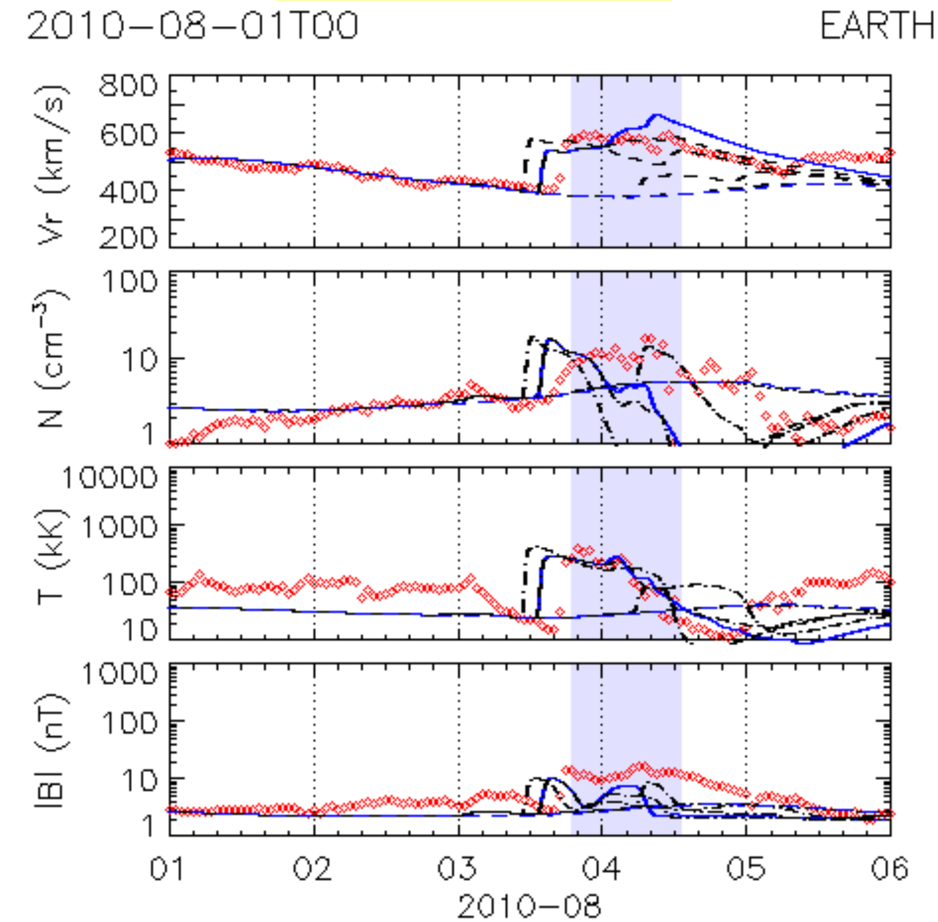

- Strength of CME-2 was reduced by weaker CME-3 (too close launch times) and thus CME-3 arrives later
- CME-3 and CME4 have ejecta at Earth

Synthetic White-Light Images of Four CMEs in 2010-08-01

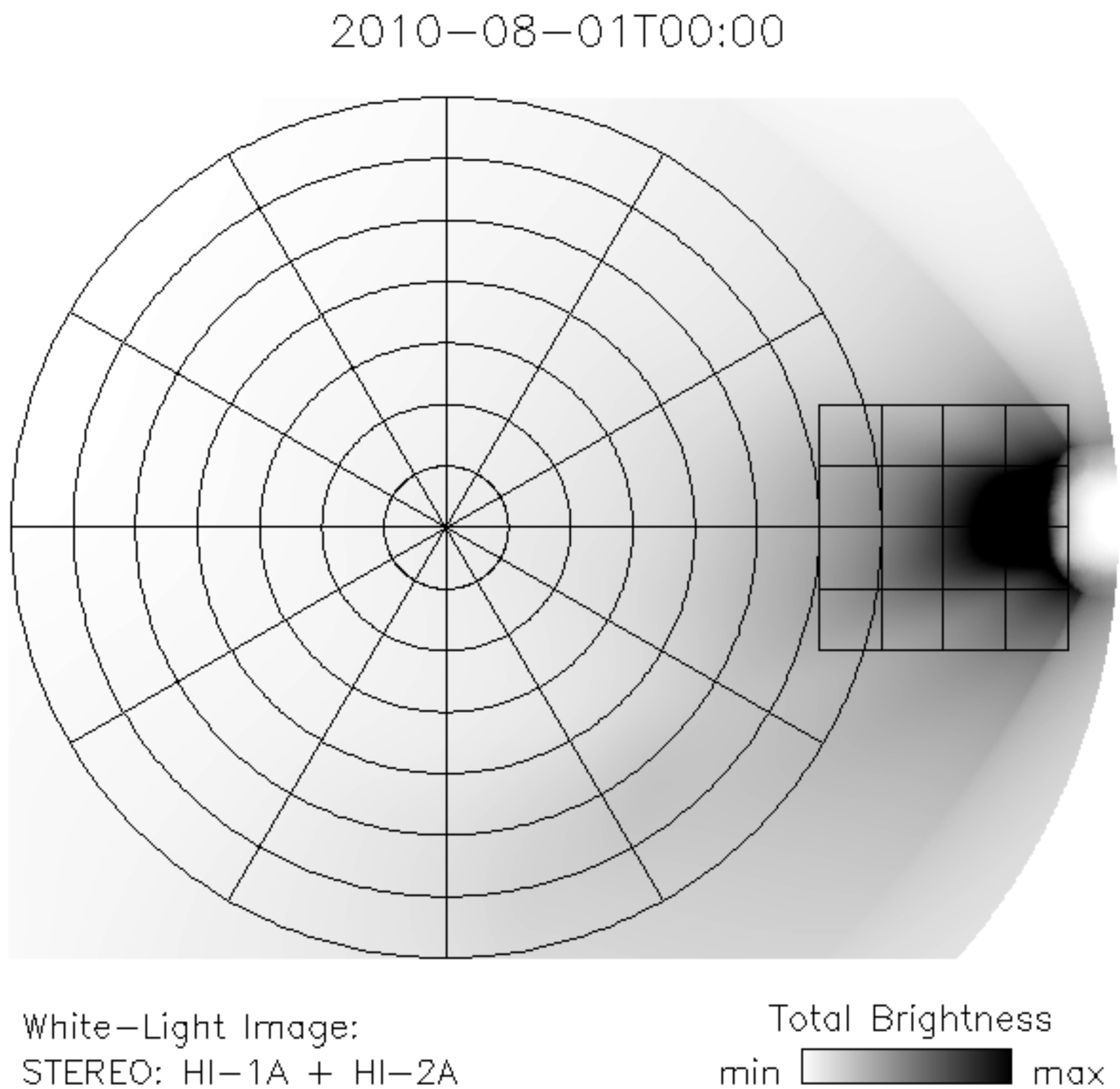

Contribution of CMEs to the J-plot (Case 1)

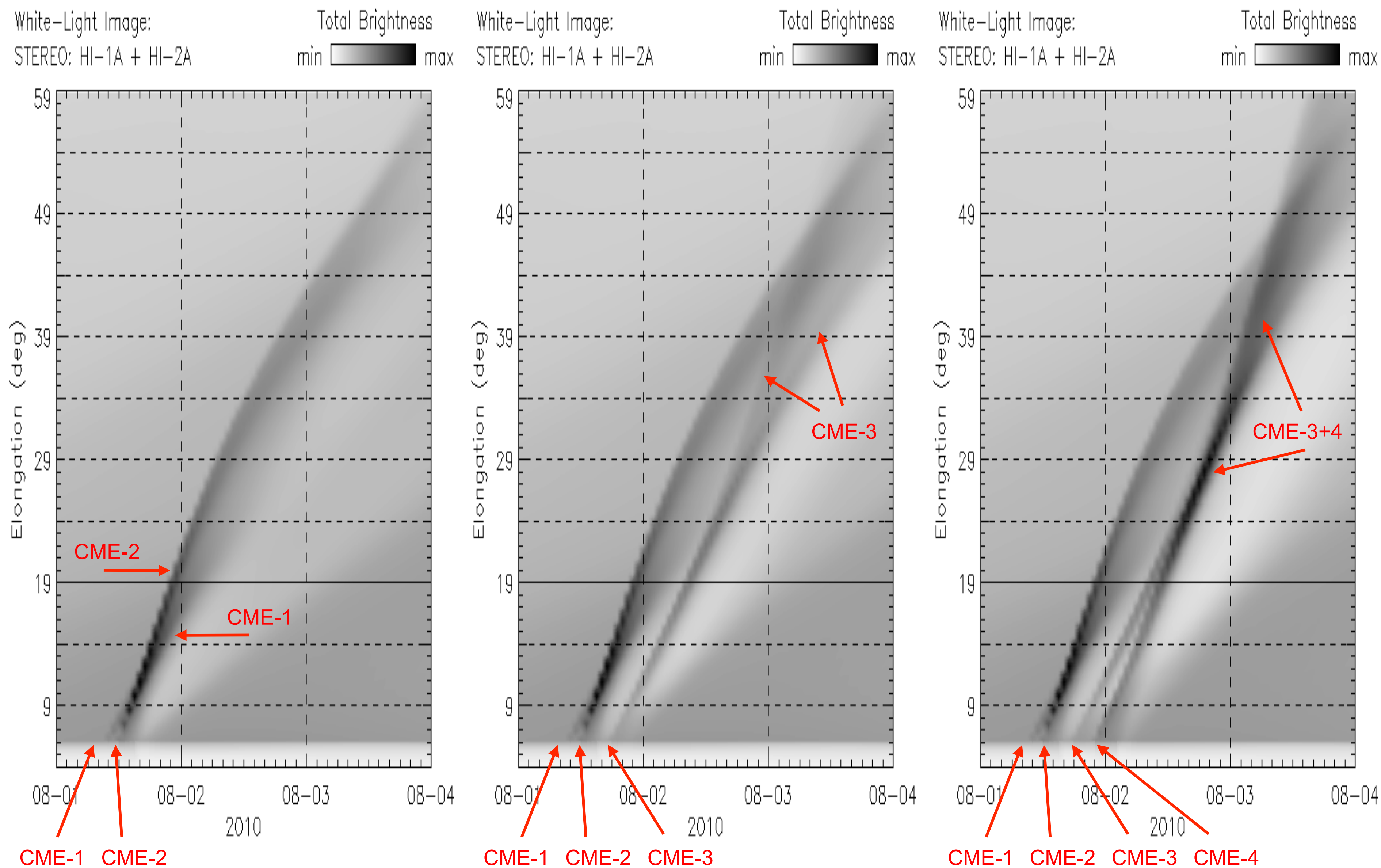

Observed Elongation-Time Plots (J-maps)

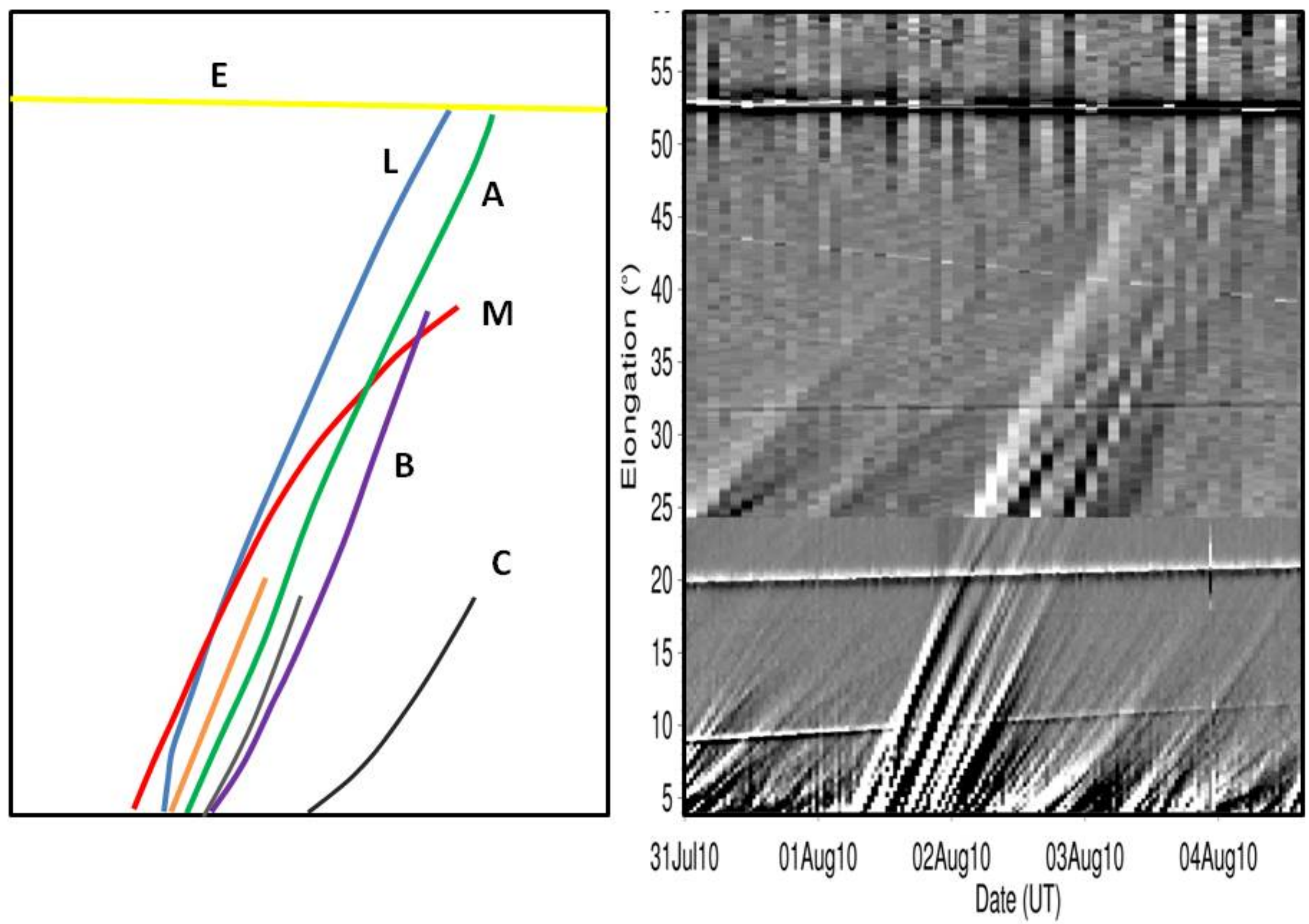

Synthetic Elongation-Time Plots (J-maps)

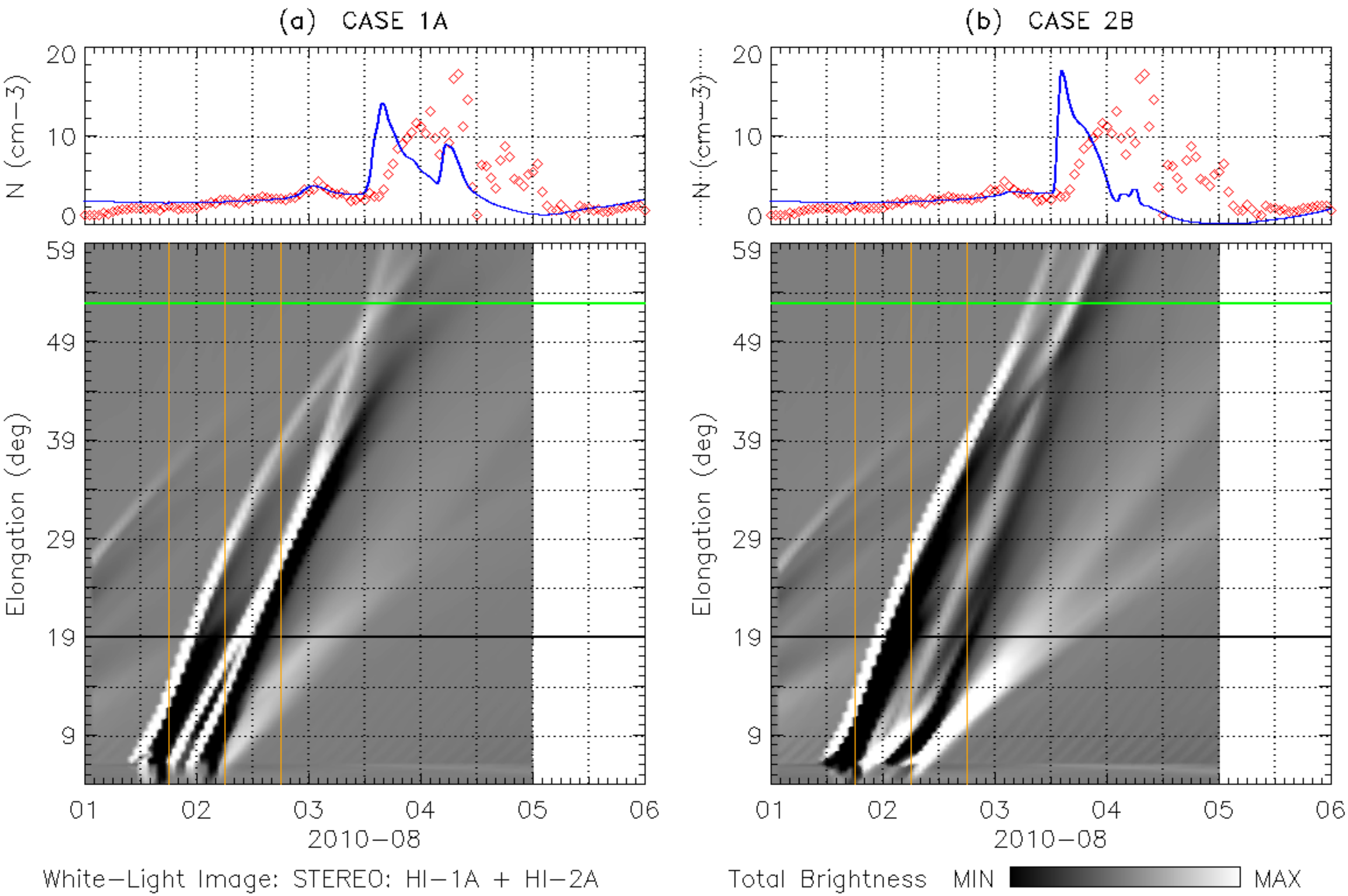

Support of SEP Modeling

Connectivity of Magnetic Field Line

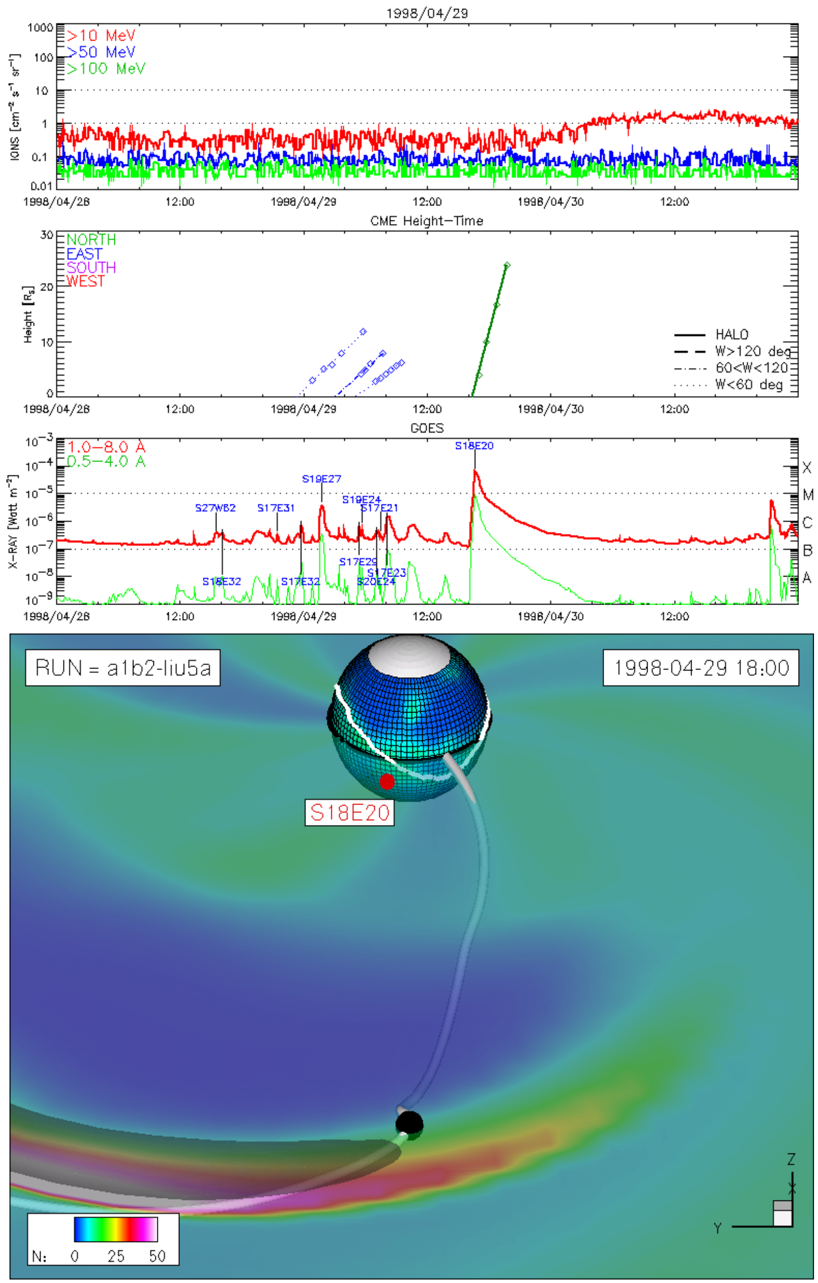

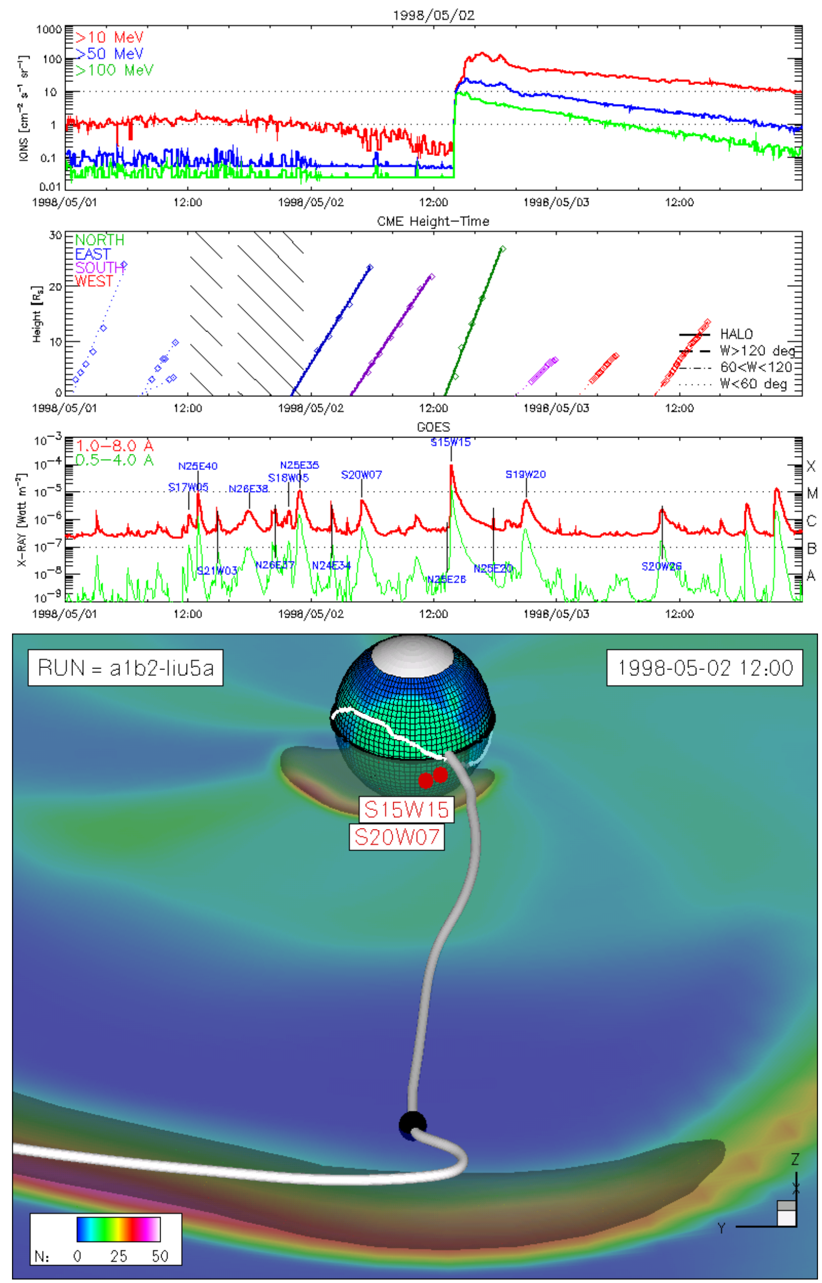

Automatic Shock Detection

Global view

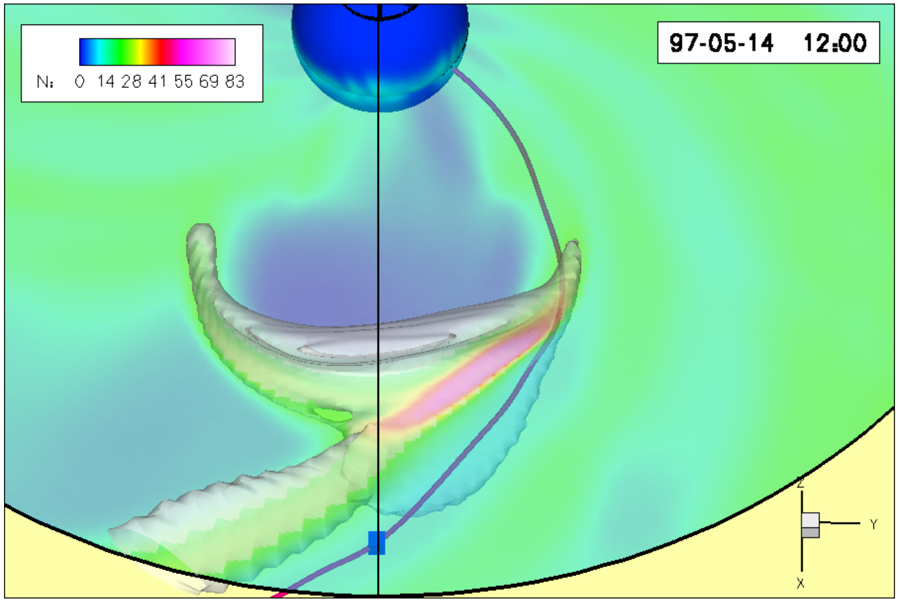

Detailed view

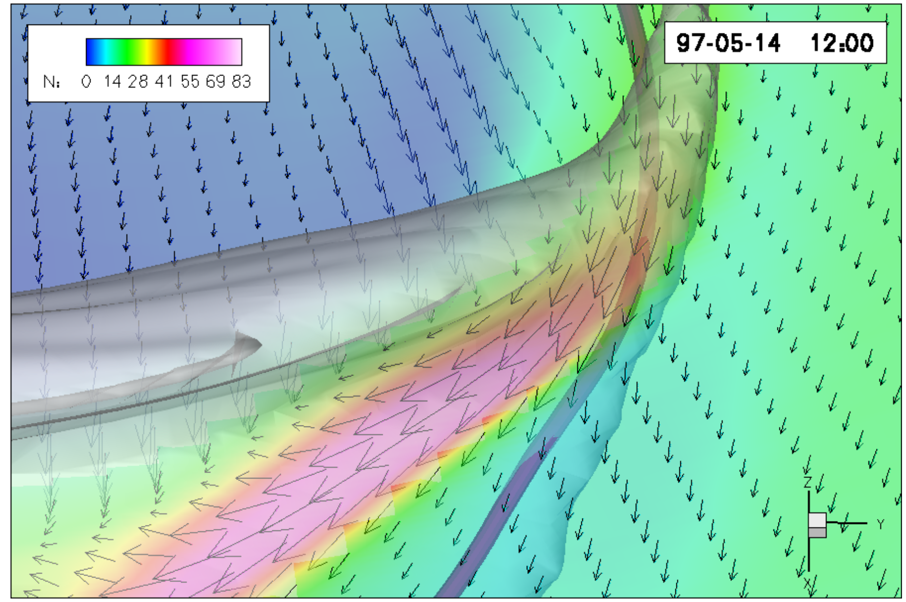

- IMF line connects geospace with an interplanetary shock under very large inclination angle because of: (1) spiraling IMF line and (2) bow-shaped shock front
- Thus determination of shock parameters from MHD values stored along the IMF line is very difficult because many numerical grid points are used across the shock structure and pre- and post-shock values are at differing solar wind

Two Shocks at the IMF Line to Earth

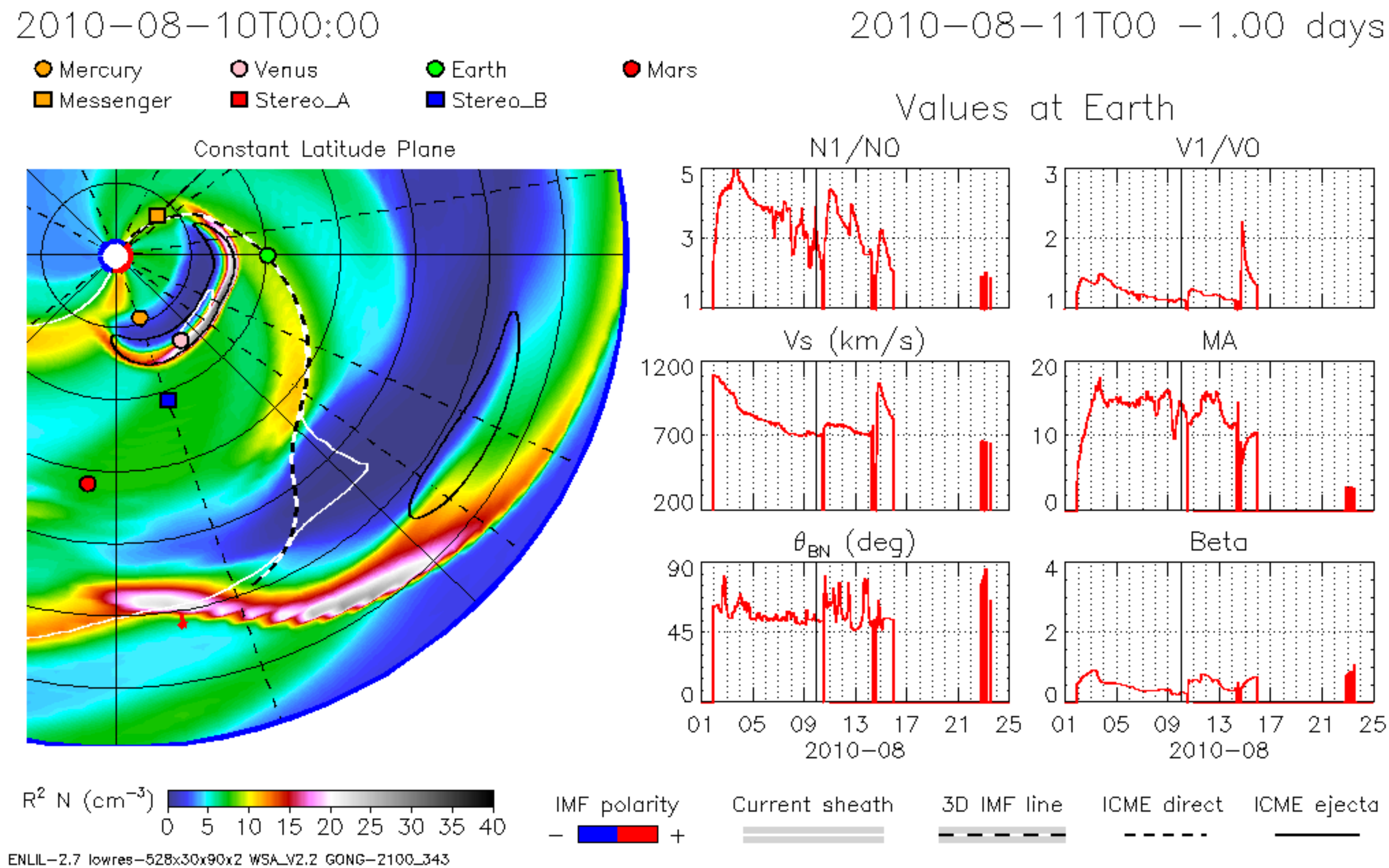

Transient+CIR Shock at the IMF Line to STA

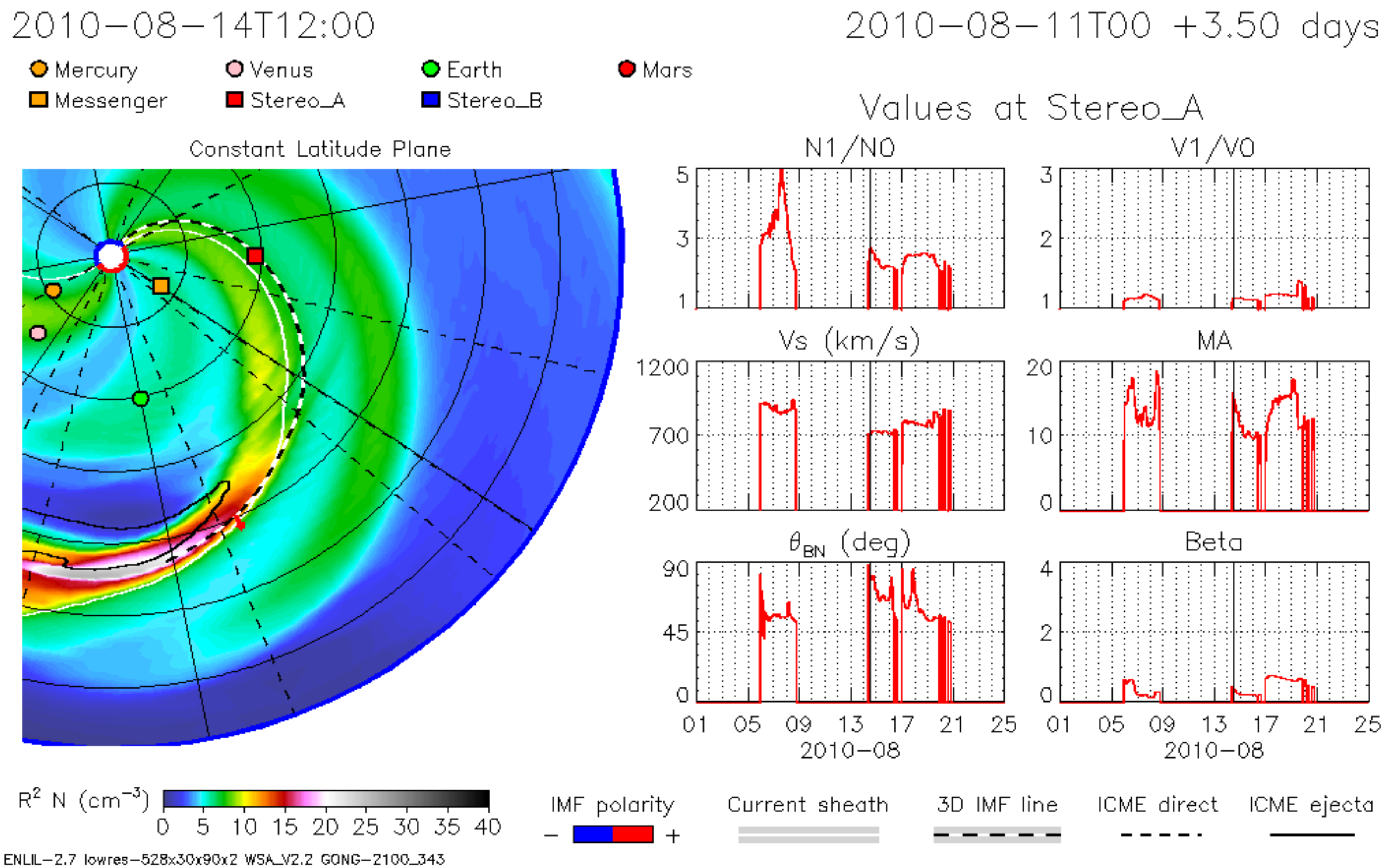

Strong Shock at the IMF Line to STB

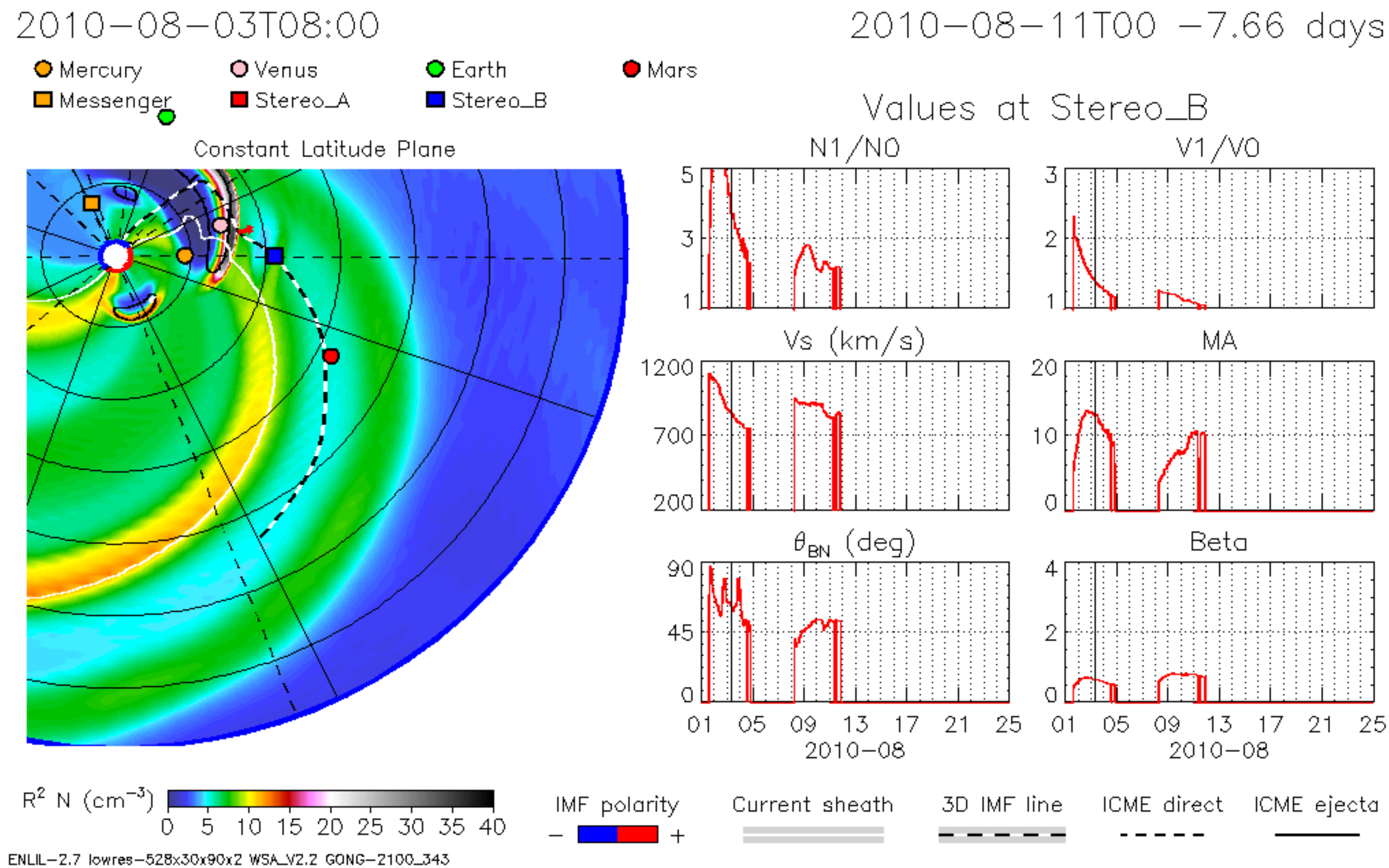

SEP Event at Earth

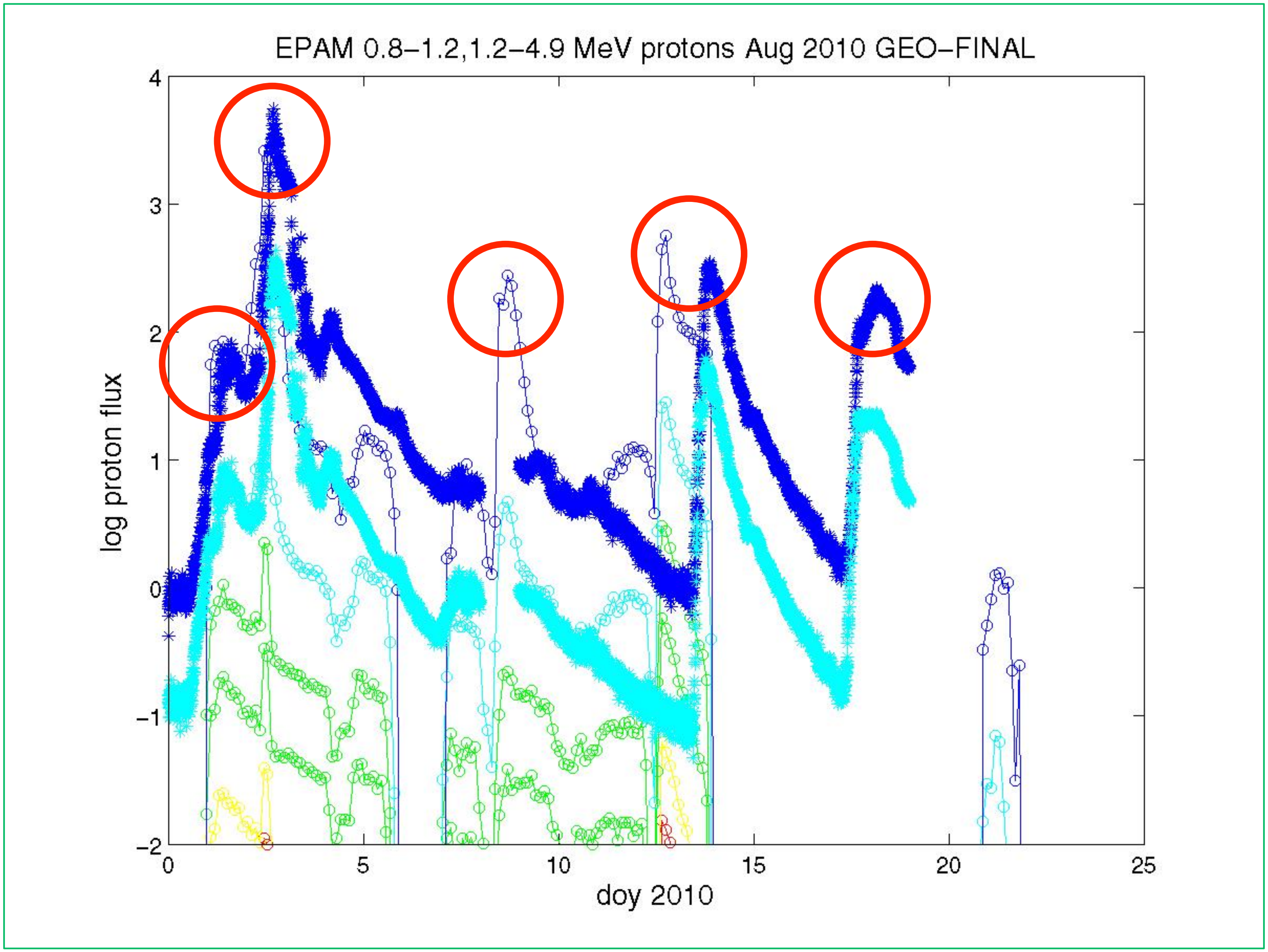

SEP Event at STEREO-B

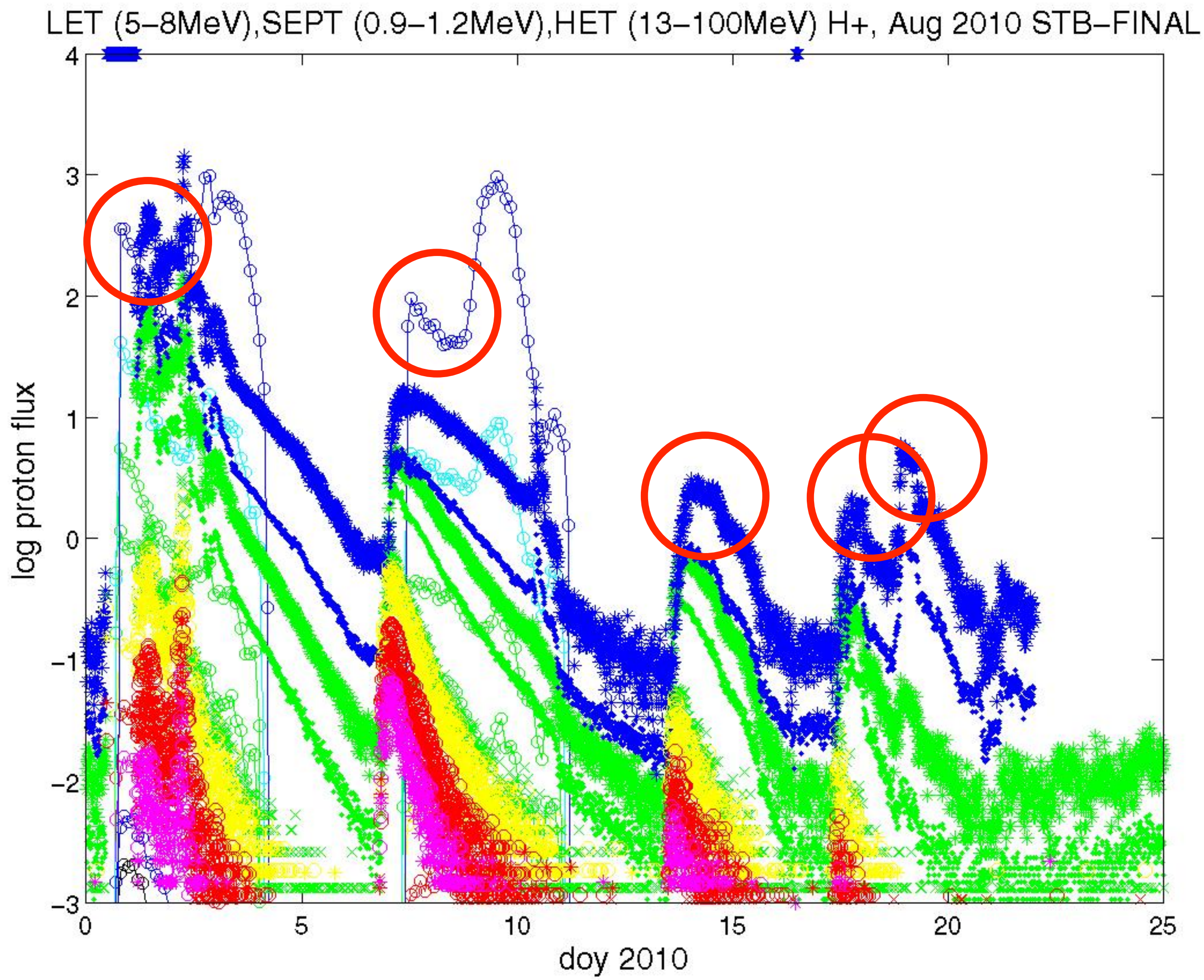

Challenges in Shocks-SEPs Modeling

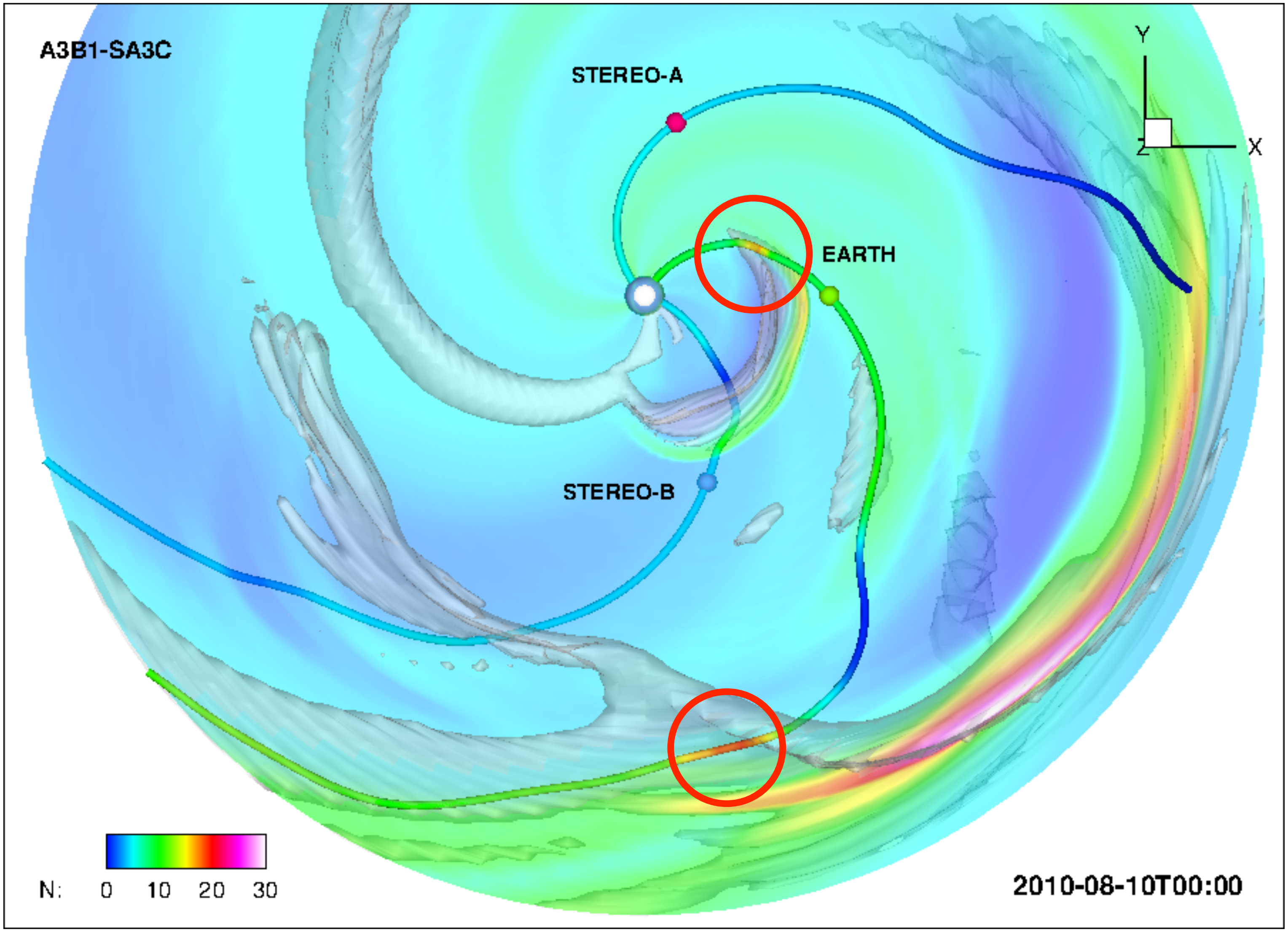

- Multiple shocks may intersects the IMF line connected to observer
- CME- and CIR-driven shocks

Input to Geospace Models

2005-05-13 ICME – Side View

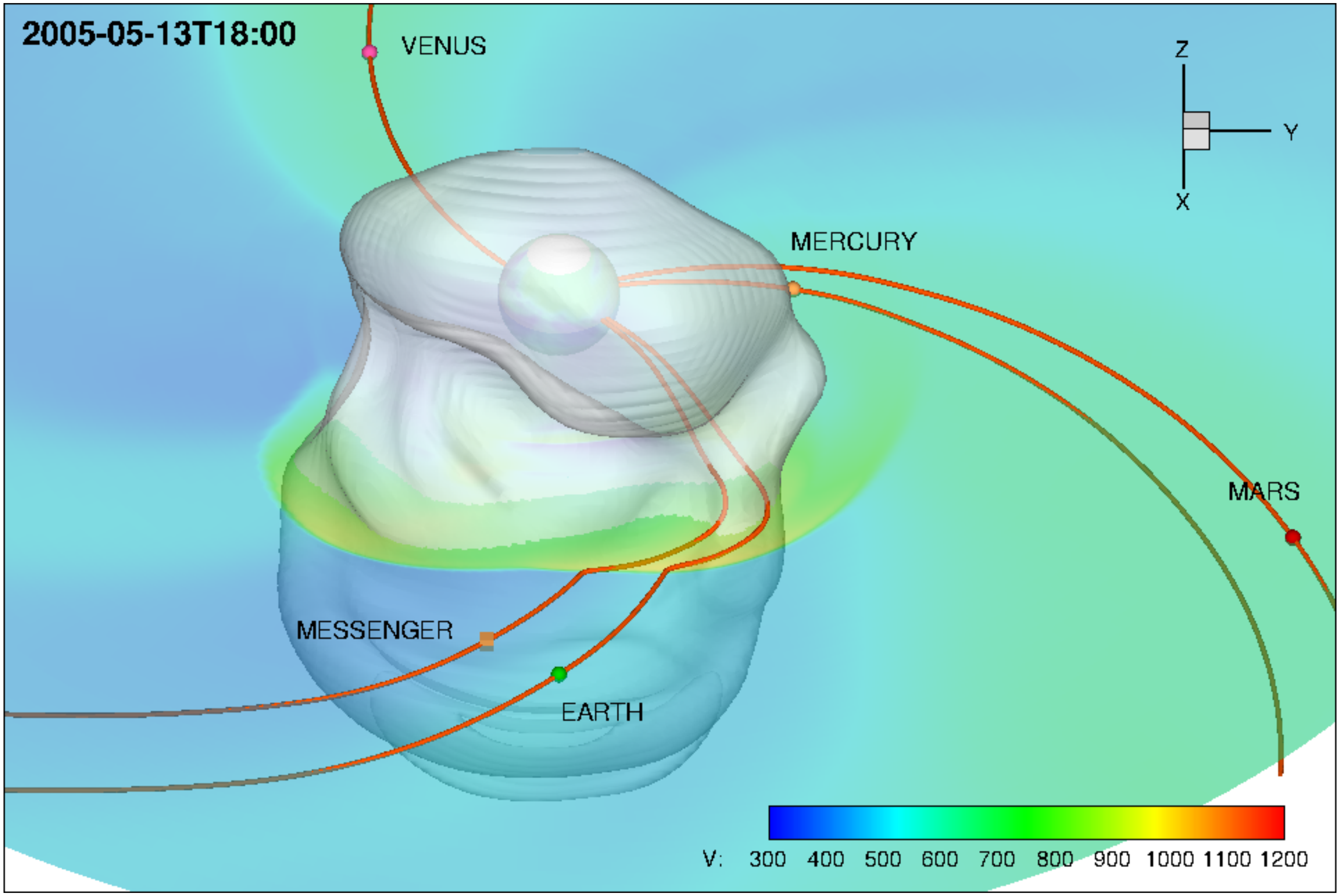

- ENLIL simulated hydrodynamic CME-like ejecta – no internal magnetic field
- ICME axis is very close to the Sun-Earth direction
- Bz cannot be generated by shock compression and/or IMF draping

2005-05-13 ICME – Front View

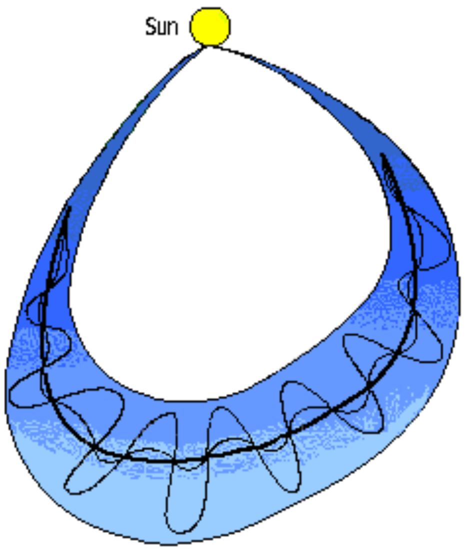

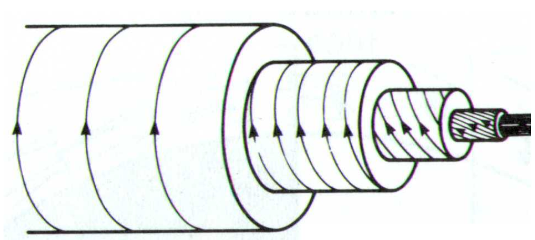

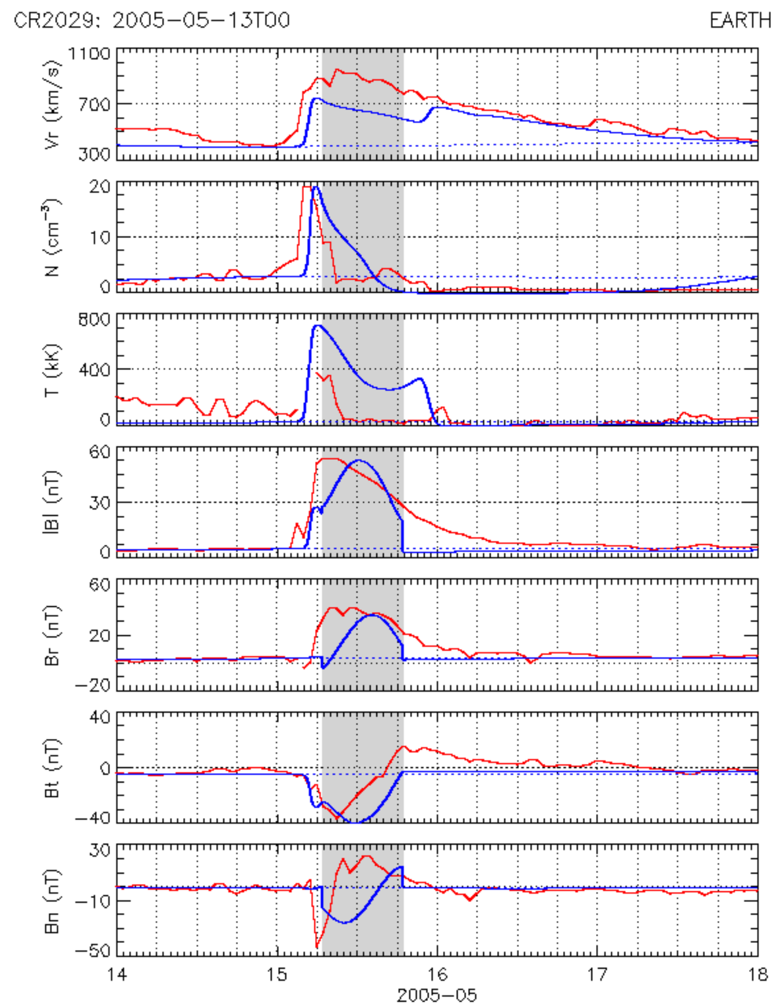

- Magnetic flux rope is described by analytic force-free (Lundquist) model.
- Temporal profiles within the traced ejecta are replaced by that solution.

Input to OpenGGCM – Geospace Response

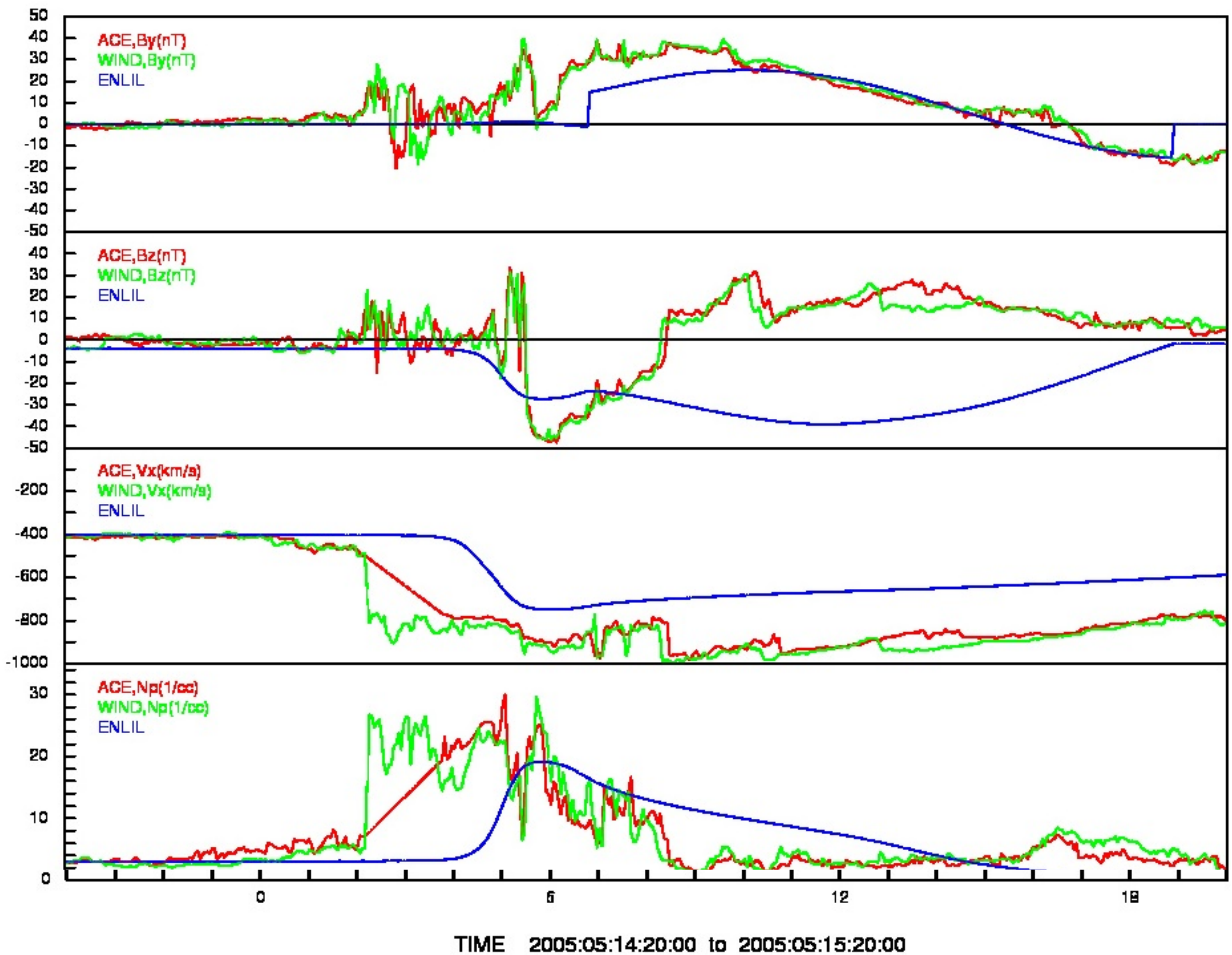

Conclusions

- ENLIL is a research code under development

- CCMC is flexible in implementation of its upgrades, user support, and feedback

- Many users wish to do “cutting-edge-research” but CCMC provides a subset of the model and limited access to model’s free parameters

- Large model calibration and validation studies are needed.

- Ensemble modeling is crucial for space weather research and forecasting